Title:

Current State of [FeFe]-Hydrogenase Research: Biodiversity and Spectroscopic Investigations

Author(s):

Henrik Land, Moritz Senger, Gustav Berggren*, and Sven T. Stripp

Citation:

"DACS Catal. 2020, 10, 13, 7069–7086 ; https://doi.org/10.1021/acscatal.0c01614"

Current State of [FeFe]-hydrogenase Research - Biodiversity and Spectroscopic Investigations

Henrik Land[1], Moritz Senger[2,3], Gustav Berggren[1*], and Sven T. Stripp[3*]

[1] Molecular Biomimetics, Department of Chemistry, Ångström Laboratory, Uppsala University, 75120 Uppsala, Sweden

[2] Physical Chemistry, Department of Chemistry, Ångström Laboratory, Uppsala University, Uppsala 75120, Sweden

[3] Bioinorganic Spectroscopy, Department of Physics, Freie Universität Berlin, Arnimallee 14, 14195 Berlin, Germany

* To whom correspondence should be addressed:

gustav.berggren@kemi.uu.se and sven.stripp@fu-berlin.de

Keywords:

Metalloenzymes, Iron-Sulfur Enzymes, Catalysis, Hydrogen Turnover, Proton-coupled Electron Transfer, Phylogenetics, Bioinorganic Chemistry, Biophysics

Table of Contents

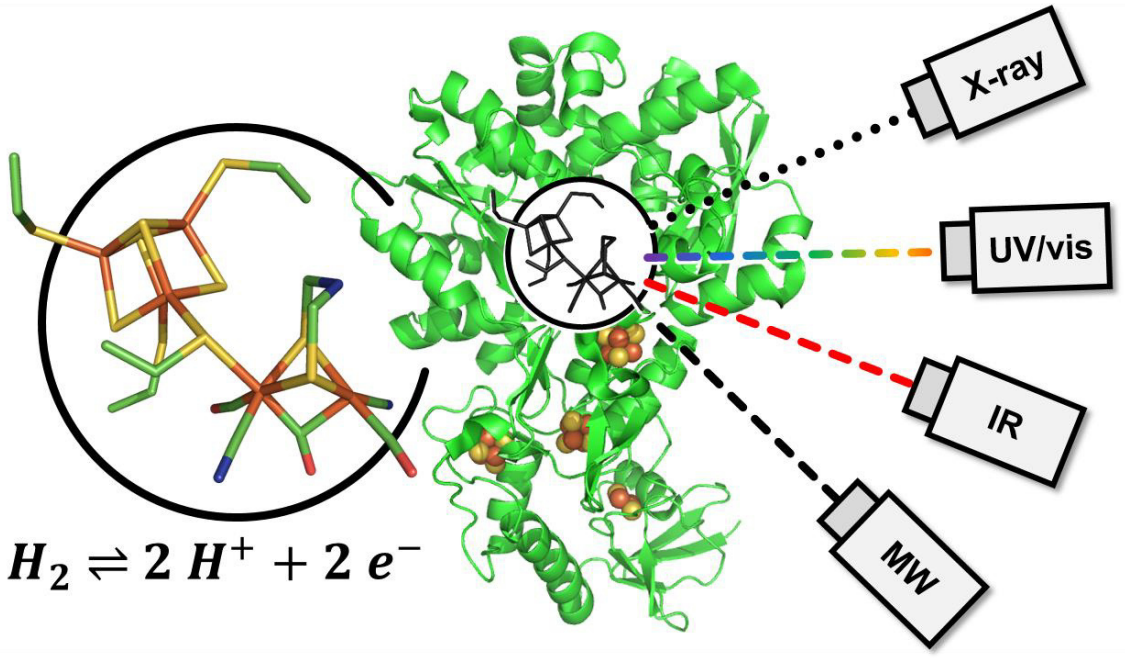

Abstract

Hydrogenases are redox enzymes that catalyze the conversion of protons and molecular hydrogen (H_2). Based on the composition of the active site cofactor, the monometallic [Fe]-hydrogenase is distinguished from the bimetallic [NiFe]- or [FeFe]-hydrogenase. The latter has been reported with particularly high turnover activities for both H_2 release and H_2 oxidation, notably at neutral pH, ambient temperatures, and negligible electric overpotential. Due to these properties, [FeFe]-hydrogenase represents the 'gold standard' in enzymatic hydrogen turnover. Understanding hydrogenase chemistry is crucial for the design of transition metal complexes that serve as potentially sustainable proton reduction or H_2 oxidation catalysts, *e.g.* in electrolytic devices or fuel cells.

Even 20 years after the crystal structures of [FeFe]-hydrogenase have been published, several aspects of biological hydrogen turnover are heatedly discussed. In this perspective, we give an overview on how the diversity of naturally occurring and artificially prepared, semi-synthetic [FeFe]-hydrogenases deepens our understanding of hydrogenase chemistry. In parallel, we cover recent results from biophysical techniques that go beyond the scope of conventional X-ray diffraction, EPR, and FTIR spectroscopy. Taking into account both proton transfer and electron transfer as well as the notorious sensitivity of [FeFe]-hydrogenases towards carbon monoxide, the discussion further touches upon the molecular proceedings of biological hydrogen turnover.

39 **Contents**

40 **1. Introduction** 4

41 **2. Novel Hydrogenases** 6

42 **2.1.1 On the Diversity of [FeFe]-hydrogenase** 6

43 **2.1.2 The Influence of F-clusters and Protein Environment** 9

44 **2.1.3 Isolation of Functional [FeFe]-hydrogenase** 12

45 **2.2 Artificial Maturation and Organometallic Variants** 15

46 **3. Novel Methods** 18

47 **3.1.1 Electronic Properties of the H-cluster** 18

48 **3.1.2 Vibrational Properties of the H-cluster** 21

49 **3.2 Biophysical Investigations *in cristallo*** 23

50 **3.3 The Influence of Temperature** 25

51 **3.4 Beyond Steady-state Spectroscopy** 29

52 **3.5 Biophysical Investigations *in vivo*** 32

53 **4. The Catalytic Mechanism** 34

54 **5. Concluding Remarks** 37

55 **6. Acknowledgements** 38

56 **7. References** 38

57

58

59

1. Introduction

Molecular hydrogen (H_2) is widely recognized as a green energy carrier with the potential to replace fossil fuels.[1–3] Considering our interest in a 'hydrogen society', it is important to realize that evolution has already developed an efficient economy based on H_2.[4] Iron-sulfur enzymes called hydrogenases are central to the hydrogen metabolism of numerous microorganisms as they catalyze the reversible conversion between protons and H_2.[5] Depending on the nature of the metal cofactor, hydrogenases are divided into three main classes denoted as [Fe]-, [NiFe]-, or [FeFe]-hydrogenase. The latter are particularly efficient catalysts with H_2 evolution activities surpassing 10,000 H_2/s.[6] Phylogenetically, there are indications that [FeFe]-hydrogenases could be the most recently evolved class of hydrogenase as archaea rely on [Fe]- and [NiFe]-hydrogenase whereas certain unicellular algae encode for [FeFe]-hydrogenase exclusively.[7–11] All [FeFe]-hydrogenases share a biologically unique cofactor, the hydrogen-activating 'H-cluster'. This organometallic moiety consists of a [4Fe-4S] cluster connected to a diiron site *via* a bridging cysteine (Figure 1). The low valence iron ions of the diiron site are bridged by an azadithiolate ligand (adt) and coordinated by the π-accepting, strong-field ligands cyanide (CN^-) and carbon monoxide (CO).[12,13] Details of the electronic structure and potential catalytic intermediates are discussed in **Chapter 3**. The biosynthesis of the H-cluster is a complex process that depends on a minimum of three [FeFe]-hydrogenase specific auxiliary enzymes.[7] Through the activity of two radical SAM enzymes (HydE and HydG), a pre-catalyst is assembled on a scaffold protein (HydF) and transferred to the hydrogenase apo-protein, generating the complete H-cluster.[14–17]

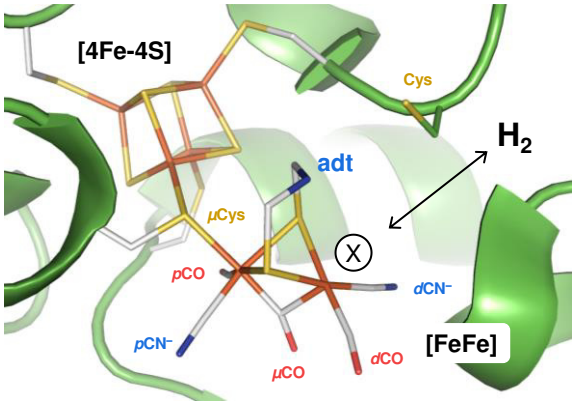

Figure 1 - The active site cofactor of [FeFe]-hydrogenase. *The H-cluster comprises a [4Fe-4S] cluster connected via a bridging cysteine (μCys) to a diiron site ([FeFe]) that is coordinated by two CN^- ligands and three CO ligands. At the open coordination site of the distal iron ion (X), gases like H_2, CO, and O_2 react with the H-cluster. The azadithiolate (adt) ligand mediates proton transfer between diiron site and protein fold, via a conserved cysteine residue (Cys) in prototypical [FeFe]-hydrogenases. Drawn using pdb coordinates 4XDC (ref. 87). Legend: p – proximal; d – distal; μ - bridging*

Stephenson & Stickland were the first to report enzymatic hydrogen activation in 1931[18] and the efforts aimed at unravelling Nature's principles for biological hydrogen conversion have accelerated quite significantly over the past 20 years. In this perspective, we cover the state-of-the-art with an emphasis on recent insights gained by studying 'new' [FeFe]-hydrogenases, derived from both biodiversity and artificial enzymes featuring synthetically modified cofactors (**Chapter 2**). Furthermore, we review trends in the spectroscopic analysis of [FeFe]-hydrogenase including transient approaches and whole-cell spectroscopy (**Chapter 3**). Our perspective will close on a brief note on the catalytic mechanism of [FeFe]-hydrogenase (**Chapter 4**).

2. Novel Hydrogenases

[FeFe]-hydrogenases are widely used as inspiration for the design of molecular catalysts and it is crucial to understand their catalytic design principles. However, only a fraction of the known [FeFe]-hydrogenases have been characterized and our knowledge on how the reactivity of the H-cluster is influenced by the protein fold in general and the active site pocket in particular is fragmentary at best. Truncation and site-directed mutation studies have been a powerful tool in this context but typically result in a loss of function.[19] In order to achieve a deeper understanding of biological hydrogen turnover, the biodiversity of [FeFe]-hydrogenase needs to be explored.

2.1.1 On the Diversity of [FeFe]-hydrogenase

Several studies of [FeFe]-hydrogenase biodiversity have been published, unfortunately with inconsistent naming conventions.[7–9,20–23] Herein, we provide a comprehensive summary of all [FeFe]-hydrogenase sub-classes identified to date, organized based on their domain structure and following the naming convention put forward by Jacques Meyer, Calusinska *et al.*, and Peters *et al.* (Figure 2).[7–9]

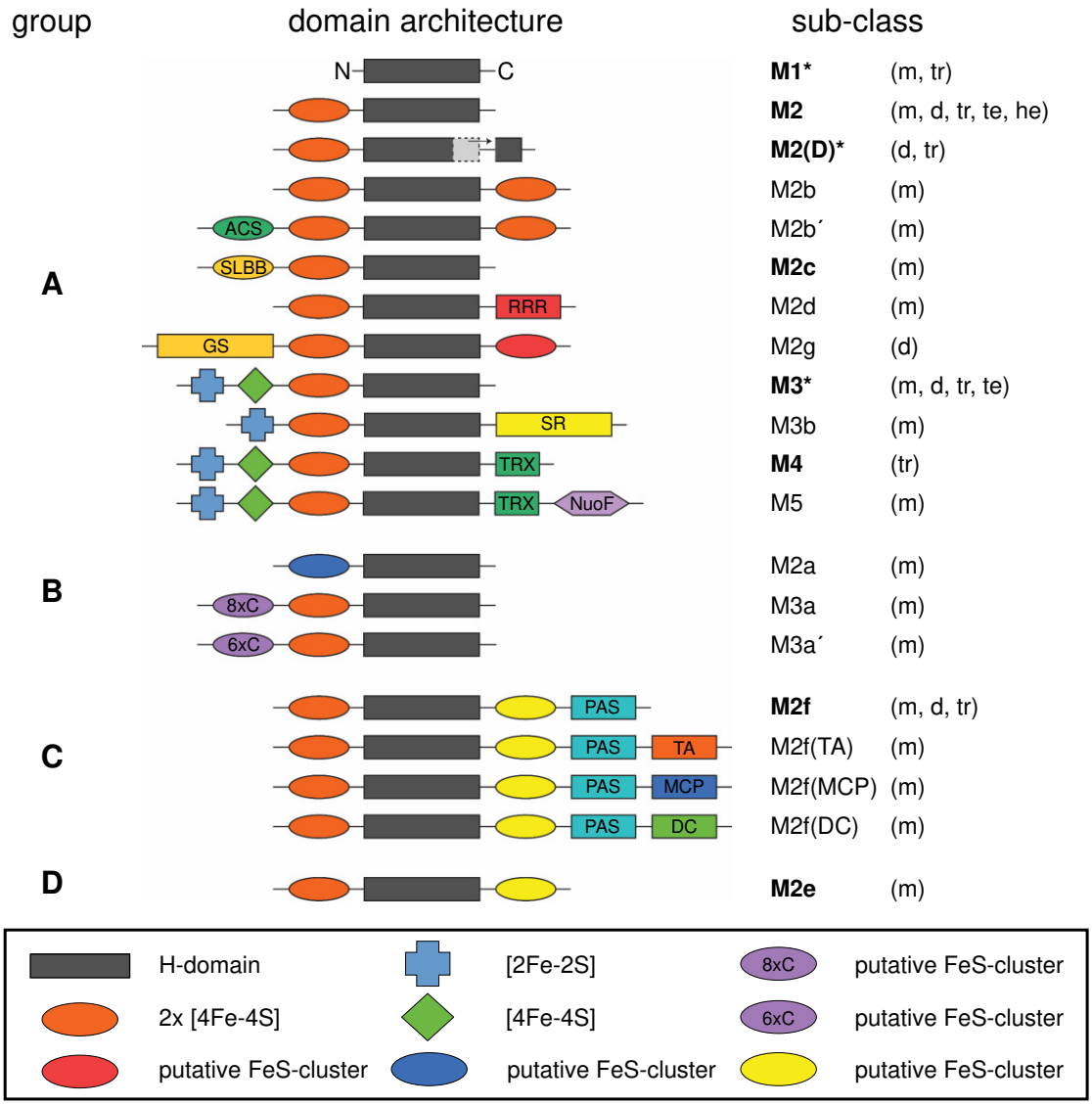

Figure 2 - Biodiversity of [FeFe]-hydrogenase. *Domain architecture of the catalytic subunit of all known [FeFe]-hydrogenase groups A – D. Sub-classes are named after their catalytic subunit where 'M' stands for monomeric and the number is indicative of size. The lower-case letter reflects that many sub-classes have been added over the years. Sub-classes in bold indicate some degree of characterization whereas sub-classes with a crystal structure are marked (*). Abbreviations in parenthesis show in which quarternary structural variations the sub-class occurs (i.e., monomeric (m), dimeric (d), trimeric (tr), tetrameric (te) and hexameric (he)). Legend: acetyl-CoA synthase binding domain (ACS), soluble-ligand-binding β-grasp binding domain (SLBB), rubredoxin-rubrerythrin-rubredoxin binding domain (RRR), glutamate synthase (GS), sulfite reductase (SR), thioredoxin (TRX), NADH:ubiquinone oxidoreductase chain F (NuoF), Per-Arnt-Sim domain (PAS), transcriptional activator (TA), methyl-accepting chemotaxis protein (MCP), diguanylate cyclase (DC).*

[FeFe]-hydrogenases can be separated into four distinct phylogenetic groups A – D (Figure 2). Group A consists of prototypical and bifurcating [FeFe]-hydrogenases. In nature, prototypical [FeFe]-hydrogenases perform hydrogen turnover using ferredoxin as redox partner while bifurcating [FeFe]-hydrogenases perform the same reaction using both ferredoxin and NAD(H) as electron donor/acceptor.[24–26] Electron bifurcation is a mechanism of biological energy conservation in which exergonic and endergonic redox reactions are coupled to circumvent thermodynamic barriers[27–29], *e.g.* in the hydrogen turnover of the [FeFe]-hydrogenase from *Thermotoga maritima* (*Tm*HydABC)[30] or *Desulfovibrio fructosovorans* (*Df*Hnd).[31] Group A comprises the best characterized and catalytically most active enzymes such as the [FeFe]-hydrogenase from *Chlamydomonas reinhardtii* (*Cr*HydA1, sub-class M1),[32] *Desulfovibrio desulfuricans* (*Dd*HydAB, often referred to as *Dd*H, sub-class M2(d)),[33] and *Clostridium pasteurianum* and *acetobutylicum* (*Cp*HydA1 and *Ca*HydA1, referred to as *Cp*I and *Ca*I, sub-class M3).[34] Group B is phylogenetically distinct although its three sub-classes show similar amino acid motifs around the H-cluster as Group A [FeFe]-hydrogenases. As no representative example of Group B has been characterized so far, distinct differences between Group A and Group B [FeFe]-hydrogenase remain to be identified. Group C has been classified as 'sensory' based on the presence of a PAS domain (Figure 2).[8,22] Moreover, genes encoding Group C enzymes are commonly found upstream from known H_2-producing [FeFe]-hydrogenases. The biochemical characterization of the M2f-type [FeFe]-hydrogenase from *T. maritima* (*Tm*HydS) further supports the notion of a sensory function as it shows modest catalytic rates and an apparent high sensitivity towards H_2.[35] The closely related sub-class M2e (Group D) have a similar gene localization and domain structure to M2f-type enzymes, suggestive of a similar physiological function (Figure 2). However, the lack of a PAS domain in combination with several differences in the active site amino acid composition makes their biological function

unclear at the moment.[8] One enzyme from this sub-class, derived from *Thermoanaerobacter mathranii* (*Tam*HydA) has recently been characterized but further investigation is needed.[36]

2.1.2 The Influence of F-clusters and Protein Environment

The protein environment has a dramatic impact on the activity of the H-cluster, *e.g.* achieved through the influence of additional iron-sulfur clusters, well-controlled proton transfer, Lewis acid/base interactions in the active site, and through modulations of the electron density distribution across the active site. [FeFe]-hydrogenase carries up to five additional iron-sulfur clusters including the M4 sub-class that carries an additional C-terminal cluster in the TRX domain (Figure 2).[22] These ferredoxin-type 'F-clusters' act as a molecular wire through the protein and ensure efficient electron transfer between biological redox partners and the H-cluster (Figure 3). The part of the enzyme that binds the F-clusters is commonly referred to as the 'F-domain' in contrast to the 'H-domain' that exclusively comprises the H-cluster. The F-clusters have a significant influence on the overall reactivity of the hydrogenase. This has been elucidated in the case of the two closely related M3-type enzymes from *Cp*I and *Ca*I as well as the sub-class M2 enzymes from *Megasphaera elsdenii* (*Me*HydA) and *Dd*H.[37–40] In the latter case, redox and pH titrations combined with FTIR and EPR spectroscopy revealed that the redox equilibrium of the diiron site is influenced by the oxidation state of the F-clusters.[39] Parallel studies of *Ca*I and *Me*HydA have shown that the F-clusters affect the catalytic bias of the enzyme. In both cases, removal of the F-domain resulted in enzymes favoring H_2 release following a significant drop in H_2 oxidation rates.[37,38]

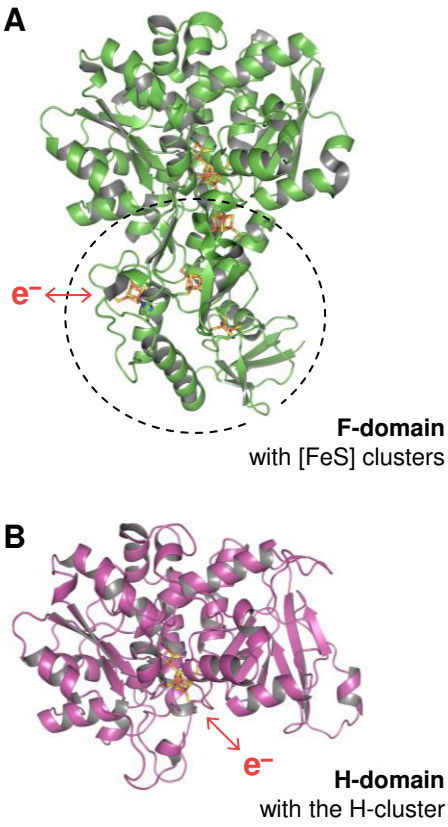

172

173 ***Figure 3 - Electron transfer and domain architecture of [FeFe]-hydrogenase.*** ***(A)*** *Crystal*
174 *structure of CpI (M3) drawn using pdb coordinates 4XDC (ref. 87). The F-domain (dashed*
175 *circle) carries three [4Fe-4S] clusters and a single [2Fe-2S] clusters that facilitate electron*
176 *transfer between H-cluster and the protein surface.* ***(B)*** *Homology model of CrHydA1 (M1).*
177 *Here, the F-domain is missing and electrons are injected directly into the H-cluster.*

178

179 The activity of [FeFe]-hydrogenase is additionally influenced by the mass transfer of gases
180 (*e.g.*, H_2, O_2, or CO) and proton transfer. Molecular dynamics simulations proposed a number
181 of putative gas channels[41] and site-directed mutagenesis could slow down O_2 inactivation in
182 individual studies.[42] However, experimental proof verifying a main trajectory for gas transfer
183 has yet to be obtained.[43] There are indications that H_2 diffuses more freely through the protein
184 than bulky gases, which suggests that there might be no such thing as a specific H_2 channel.

185 The proton transfer pathway in Group A [FeFe]-hydrogenase comprise a series of well-
186 conserved amino acid and water residues that enable proton transfer between the H-cluster and

the enzyme surface (Figure 4).[44–46] It starts at the H-cluster with a cysteine residue (C_1) responsible for proton transfer to the H-cluster and continues with a serine (S_1), glutamate (E_1, E_2), and an arginine residue (R).[47,48] A methionine 'above' the H-cluster (M_2) was discussed as hydrogen-bonding partner to the adt ligand possibly providing an alternative proton transfer trajectory.[49] However, in Group C [FeFe]-hydrogenases neither cysteine C_1 nor methionine M_2 are conserved.[35] Another putative proton transfer pathway was suggested to involve a conserved lysine residue (K) close to the distal iron ion.[13] Together, this implies that more investigations on possible proton transfer pathways in [FeFe]-hydrogenase are needed, in particular to understand the chemistry of the Group C and Group D enzymes.

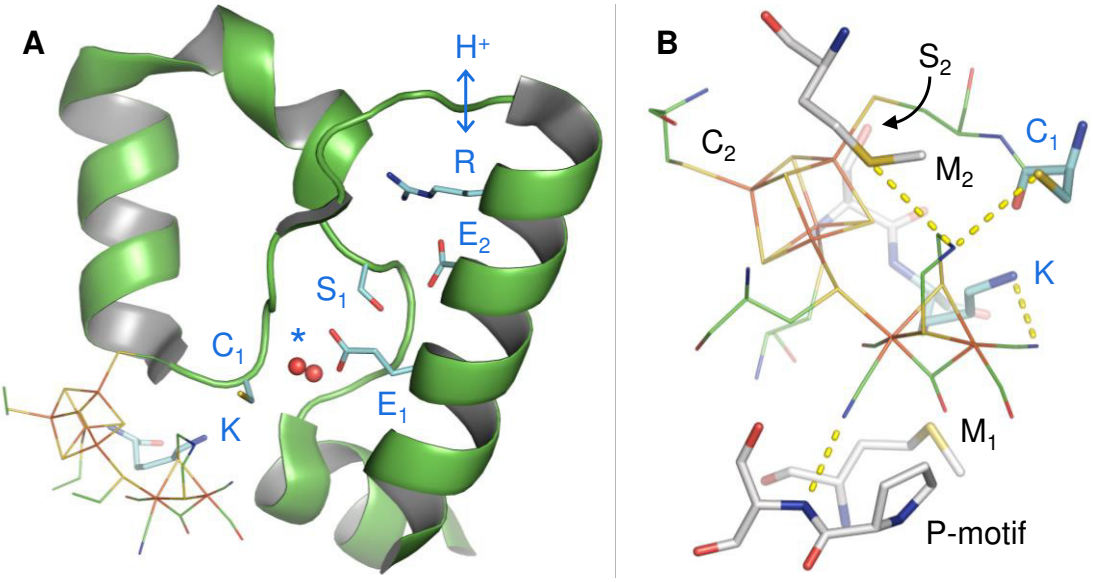

Figure 4 - Proton transfer pathway and active site niche of [FeFe]-hydrogenase. Crystal structure of *Cp*I (M3), drawn using pdb coordinates 4XDC (ref. 87). **(A)** A conserved set of amino acid residues (blue sticks and labels) and water molecules (*) facilitates bidirectional proton transfer. Alternatively, lysine residue K was discussed to be involved in proton transfer. **(B)** At the diiron site, two methionine residues (M_1, M_2) and a backbone contact including a proline residue ('P-motif') influence the H-cluster geometry and catalytic bias. The identity and protonation state of amino acid residues at the [4Fe-4S] cluster (including cysteine C_2 and serine S_2) has been shown to affect the electrochemical properties of the H-cluster.

The amino acid environment of the H-cluster is suspected to play a role beyond modulating gas access and proton transfer. For example, the CN^- ligands of the H-cluster were modelled according to potential hydrogen-bonding partners, *i.e.* lysine K and a backbone contact involving a proline residue ('P-motif', *e.g.* APA in *Cr*HydA1 and *Dd*H or APS in *Cp*I and *Ca*I) close to the proximal iron ion, Fe_p (Figure 4).[19] Hydrogen bonding between K and Fe_d-CN^- is a reasonable assumption and likely to be relevant in cofactor insertion but has not been verified experimentally. In contrast, site-directed mutagenesis of the 'P-motif' had significant impact on catalytic bias and spectroscopic properties.[50] This demonstrated how the protein modulates the electron density of the diiron site through Lewis acid/base interactions with the CN^- ligands. At the [4Fe-4S] cluster, amino acid exchanges[51] and protonation differences (C_2 in Figure 4)[52] have been shown to affect the electrochemical properties of the H-cluster, and a similar effect was discussed for the orientation of a conserved serine (S_2 in Figure 4).[53] Moreover, a methionine residue below the H-cluster was suggested to promote the release of μCO into a semi-bridging or terminal position upon reduction of the diiron site (M_1 in Figure 4).[35] The conservation of this methionine is a key difference between groups A/B and C/D and has important implications for the catalytic mechanism (**Chapter 4**). Finally, it has also been proposed that differences in the 'polarity' of the active site, enables tuning of [FeFe]-hydrogenases towards either H_2 release or H_2 oxidation.[53]

2.1.3 Isolation of Functional [FeFe]-hydrogenase

Historically, the preparation of pure [FeFe]-hydrogenase samples has been limited by several factors. In the 1950s, enzyme isolation was limited to homologous expression, causing significant challenges depending on the source organism.[54] During the 1970s and 1980s, heterologous (over-) expression in easy-to-handle host organisms such as *Escherichia coli* or *Pichia pastoris* was developed and became the method of choice.[55,56] However, the successful expression of an active [FeFe]-hydrogenase in *E. coli* was not published until 2004, when

Posewitz *et al.* reported the co-expression of *Cr*HydA1 with the auxiliary maturases HydEFG from *C. reinhardtii*.[14] The method was then refined by using the *E. coli* strain BL21(DE3)ΔiscR in which deletion of the gene encoding the transcriptional regulator IscR stimulates iron sulfur cluster biosynthesis. This resulted in a ten-fold increase in yield of active [FeFe]-hydrogenase compared to previous reports.[57,58] Expressing [FeFe]-hydrogenase in *C. acetobutylicum* or *Shewanella oneidensis* (*i.e.*, bacteria natively expressing HydEFG) suffered from complications in handling these organisms.[59–61] In 2013, it was shown that inactive [FeFe]-hydrogenase apo-protein can be heterologously overexpressed and artificially activated using a synthetic mimic of the cofactor (**Chapter 2.2**).[62,63] This breakthrough paved the way for a new era in [FeFe]-hydrogenase discovery. By taking advantage of the increasing amount of sequenced genomes[64], bioinformatics can identify any [FeFe]-hydrogenase encoding gene of interest, regardless of the source organism. The genes can then be codon-optimized for expression in common hosts and synthesized in a matter of days. This approach was recently explored when eight putative [FeFe]-hydrogenase genes from a range of different sub-classes were synthesized and expressed in conventional *E. coli* expression strains, notably without co-expression of HydEFG.[36] Active hydrogenase was generated through addition of synthetic cofactor mimics to the cell suspension.

Outlook. Several aspects motivate the discovery of novel [FeFe]-hydrogenases. *Firstly*, mechanistic studies of [FeFe]-hydrogenase are necessary to understand their complex chemistry and to aid the development of efficient biomimetic catalysts. As previously mentioned, the vast majority of the characterized [FeFe]-hydrogenases originate from Group A. Although the active site architecture in this group is conserved, these enzymes still exhibit clear differences in catalytic behavior. Rates for H_2 release and H_2 oxidation differ by a factor of 500 and 15,000, respectively, underscoring the influence of the non-catalytic domains on the activity of the enzyme. But also between the closely related [FeFe]-hydrogenases within

the same sub-class of Group A H_2 release rates differ up to 40 times,[53,65–67] suggesting that even a detailed discrimination based on differences in domain structure and active site architecture does not allow for an impeccable prediction of catalytic activity. Clearly, aspects of the molecular determinants of [FeFe]-hydrogenase turnover kinetics are poorly understood. Moving forward, comparative studies of different [FeFe]-hydrogenases from the same organism, as exemplified by a recent report on *Cp*I – III by Artz *et al.*, can be expected to shed light into factors fine-tuning the reactivity of [FeFe]-hydrogenase.[53] In the context of molecular design, studies of point mutants and truncated [FeFe]-hydrogenases has provided critical insight into protein/cofactor interplay primarily through loss-of-function observations.[49,68] Other variations critically affect the catalytic bias.[50,69] Complementing such work with gain-of-function studies is expected to provide a wealth of additional data, *e.g. via* domain-swapping and/or the transformation of low-activity Group C or Group D enzymes to an enzyme displaying activities *on par* with Group A [FeFe]-hydrogenase.

Secondly, the understanding of biological hydrogen metabolism is still rather limited. From an environmental and biotechnological perspective, the organisms capable of metabolizing H_2 needs to be better understood. This is also relevant from a medical perspective since many of these organisms are involved in human pathogenesis.[11] Beyond hydrogen turnover activity, the bifurcating, multimeric [FeFe]-hydrogenases of Group A are interesting for the study of metabolic networks, *e.g.* involving NAD(P)H and CO_2 conversion.[26–29] Moreover, *Df*Hnd (sub-class M3) and the [FeFe]-hydrogenase from *Clostridium beijerinckii* (*Cb*A5H, sub-class M2c) appears to display a unique tolerance towards O_2.[31,70] These observations underscore the potential of exploring hitherto uncharacterized sub-classes in efforts to discover enzymes with unprecedented activities and properties.

Thirdly, there is a great need to increase the toolbox of available [FeFe]-hydrogenases so that the best possible candidates can be identified with regards to catalytic performance and O_2

tolerance. These enzymes can then be optimized, *e.g.* through directed evolution and applied in industrial H_2 production or in biotechnological devices such as fuel cells. In the next chapter, we will discuss modification of the active site cofactor beyond the scope of nature.

2.2 Artificial Maturation and Organometallic Variants

The biosynthesis of the H-cluster proceeds *via* a discrete intermediate containing the [4Fe-4S] cluster but lacking the diiron site.[71,72] This intermediate is commonly referred to as 'apo-protein' despite carrying at least one metal center already. As hydrogenase apo-protein is readily isolated *via* heterologous expression in the absence of HydEFG, the assembly line could be hijacked through the introduction of synthetic analogues of the diiron site ('artificial maturation') enabling the preparation of semi-synthetic [FeFe]-hydrogenase (Figure 5).[62,63] More recently, this strategy has been utilized to identify possible intermediates in the assembly of the pre-catalyst.[73–75] Arguably, the main impact of artificial maturation to-date has been the simplified preparation of the active enzyme[30,66] including site-selective isotopologues,[76–78] which also facilitates rapid screening protocols.[36] Another important aspect is the preparation of [FeFe]-hydrogenases in which the diiron site is synthetically modified in order to generate non-natural H-clusters and enzymes with new properties.[79–82]

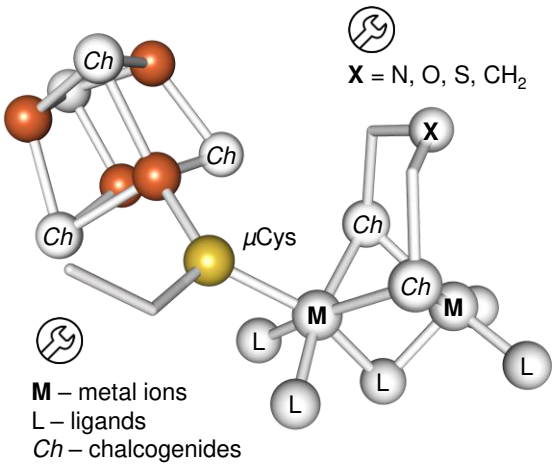

298

299 ***Figure 5 - The H-cluster as a toolbox.*** *Several organometallic variants comprising non-*
300 *natural cofactors have been reported. Modifications include different metal ions (M) and metal*
301 *ligands (L), the replacement of sulfur against selenium (chalcogenides, Ch), and different*
302 *variations of the dithiolate headgroup (X).*

303

304 In the case of Group A [FeFe]-hydrogenase, the active site cavity has been extensively explored
305 through site-directed mutagenesis (**Chapter 2.1.2**).[49–52] Of particular note in the context of
306 organometallic variants is the critical importance of hydrogen-bonding interactions between C_1
307 (Figure 4) and the central nitrogen atom of the adt group.[45] Artificial maturation has enabled
308 detailed studies of this proton transfer pathway and facilitated the discovery of a number of
309 proton-coupled electron transfer events relevant to the catalytic cycle of the H-cluster (**Chapter**
310 **4**), *i.e.* through manipulations of the diiron site rather than the protein (Figure 5). For example,
311 diiron complexes that carry propanethiolate (pdt) or oxodithiolate (odt) ligands instead of the
312 natural adt ligand can be incorporated into the apo-protein with good yields. Such variants
313 showed very specific turnover characteristics and allowed locking the H-cluster in specific
314 oxidation states (**Chapter 3.1**).[62,63] Numerous other organometallic variants have been
315 reported, documenting modifications all across the H-cluster (Figure 5). The iron ions have
316 been replaced by ruthenium, resulting in the formation of a [RuRu] terminal hydride species
317 that appears highly stable.[83] The chalcogens have been changed from sulfur to selenium in both

318 the [4Fe-4S] cluster as well as the diiron site.[84,85] The latter variant showed a shift in catalytic
319 bias towards H_2 release, but also suffered from a significant decrease in cofactor stability.
320 Modifications of the diatomic ligands revealed that monocyanide variants of the H-cluster
321 retain remarkable residual activity both *in vitro* and in whole cells.[85–89]

322 **Outlook:** The preparation of organometallic variants will undoubtedly continue contributing
323 to our mechanistic understanding of [FeFe]-hydrogenase. The preparation of modified H-
324 clusters outcompeting the native cofactor remains a significant challenge, although the
325 selenium analogue appears to improve H_2 release activity.[84,85] It is noteworthy that synthetic
326 modification of the diiron site have a dramatic effect on the reactivity towards known
327 inhibitors.[89] Thus, it arguably provides a convenient route towards more stable catalysts. In
328 parallel to the enzymology aspect, the generation of highly active, semi-synthetic [FeFe]-
329 hydrogenases is of particular relevance in the context of designing small molecule systems.
330 Since the structural elucidation of the H-cluster two decades ago,[12,13] the design and
331 characterization of synthetic diiron complexes has been a highly active research field, and
332 several comprehensive reviews have been published on the topic.[90–92] Historically, this work
333 has been critical, *e.g.* in assigning the nature of the diatomic ligands, identifying the nature of
334 the bridgehead atom, highlighting the importance of acid/base residues in the vicinity of the
335 metal sites, and mapping out the reactivity of terminal *vs.* bridging hydrides. In solution, such
336 small molecule mimics generally display limited catalytic efficiencies; however, upon
337 incorporation into the enzyme unstable complexes are transformed into highly active catalysts.
338 This immediately underscores the importance of the [4Fe-4S] cluster and the protein
339 environment for activity (**Chapter 2.1.2**). Analogously, the catalytic properties of small
340 molecule systems can be significantly improved through the addition of redox and acid/base
341 functionalities[91–94], or by incorporating them into polymers.[95–97] In order to disentangle the
342 different effects of the protein fold on the reactivity of synthetic diiron complexes, it is highly

relevant to complement studies of different sub-classes of [FeFe]-hydrogenase with model systems featuring redox active ligands in combination with a more elaborate second coordination sphere.

3. Novel Methods

The H-cluster has been investigated by continuous-wave and pulsed EPR spectroscopic techniques as well as Mössbauer spectroscopy, nuclear resonance vibrational spectroscopy (NRVS), and nuclear magnetic resonance spectroscopy (NMR). Similarly, the CO and CN^- ligands of the H-cluster provide exquisite marker bands for FTIR spectroscopy. FTIR and EPR spectroscopy have arguably become the methods-of-choice in the field. Albeit not novel methods, these techniques are continuously employed in the identification of new states of potential catalytic relevance. In the following section, we will outline how spectroscopy has provided the foundation for our current mechanistic understanding, before describing how certain methods are used in new ways to provide even more detailed insight into H-cluster chemistry. In addition, recent data from synchrotron methods are discussed.

3.1.1 Electronic Properties of the H-cluster

The paramagnetic resting state **Hox** gives rise to a rhombic signal (g=2.10, 2.04, 2.00; see Figure 6) representing the oxidized [4Fe-4S] cluster (+2) and a mixed-valence diiron site (Fe_p(II)-Fe_d(I), +3).[98–100] The symmetry of the formally diamagnetic [4Fe-4S] cluster (*i.e.*, a pair of Fe(II)Fe(III) with S = 9/2) is broken due to spin exchange coupling with the diiron site (S = 1/2). Lubitz *et al.* noted that the strong electronic contact facilitates electron transport between [4Fe-4S] cluster and diiron site.[101] Accordingly, the putative protonation of the [4Fe-4S] cluster in **HoxH** (see below) is observable by EPR spectroscopy (Figure 6). Upon CO inhibition, spin exchange coupling is significantly enhanced in favor of the [4Fe-4S] cluster leading to an axial EPR spectrum with g = 2.05 and 2.01 in **Hox-CO** (Figure 6).[102,103] The spin polarization was recently calculated to fit an apical CO model.[104] Studying the ^{14}N hyperfine

interactions, Silakov *et al.* revealed the chemical nature of the dithiolate group resolving a long-running controversy whether its central atom is an oxygen (odt), carbon (pdt) or nitrogen atom (adt) in favor of the latter.[105] Proton-coupled electron transfer involving the amine bridgehead of the adt ligand results in the formation of the diamagnetic state **Hred** (Fe_p(I)-Fe_d(I), +2). Here, the [4Fe-4S] cluster remains oxidized.[98] Further reduction of this species gives the rhombic EPR spectrum of a [4Fe-4S] cluster (+1) characteristic for the 'super-reduced' H-cluster, **Hsred**. Often, these states are referred to as $HredH^+$ and $HsredH^+$ in literature. Recently, the EPR signature of **Hsred** (g = 2.08, 1.94, 1.87)[106,107] was re-interpreted to stem from Hhyd:red, a hydride-like H-cluster intermediate. Lorent *et al.* suggest an alternative axial EPR signature (g = 2.15, 1.86) for **Hsred**.[108] Due to spin exchange coupling, the H-cluster is EPR-silent when *only* the [4Fe-4S] cluster is reduced (**Hred´** and **Hred´-CO**).[109] More recently, an H-cluster species with a terminal hydride was discovered, the so-called hydride state (**Hhyd**).[110–112] EPR, Mössbauer, and FTIR spectroscopy identified the latter as a 'super-oxidized' diiron site (Fe_p(II)-Fe_d(II), +4) coupled to a reduced [4Fe-4S] cluster (+1), giving rise to a rhombic EPR spectrum (g = 2.07, 1.93, 1.88, see Figure 6).[110] Further, the EPR spectrum of **Hhyd** bears similarities to the inactive **Htrans** state (g = 2.06, 1.96, 1.89 as observed in *Dd*H).[106] Direct proof for the presence of a terminal hydride was presented by Reijerse *et al.* who applied NRVS on ^{57}Fe-enriched samples of *Cr*HydA1-odt investigating the low-frequency Fe_d-H^- vibration at ~730 cm^{-1} and ~670 cm^{-1}.[113] The terminal hydride was additionally identified by ^{1}H NMR.[114] Figure 7 depicts the electronic configuration of key H-cluster intermediates.

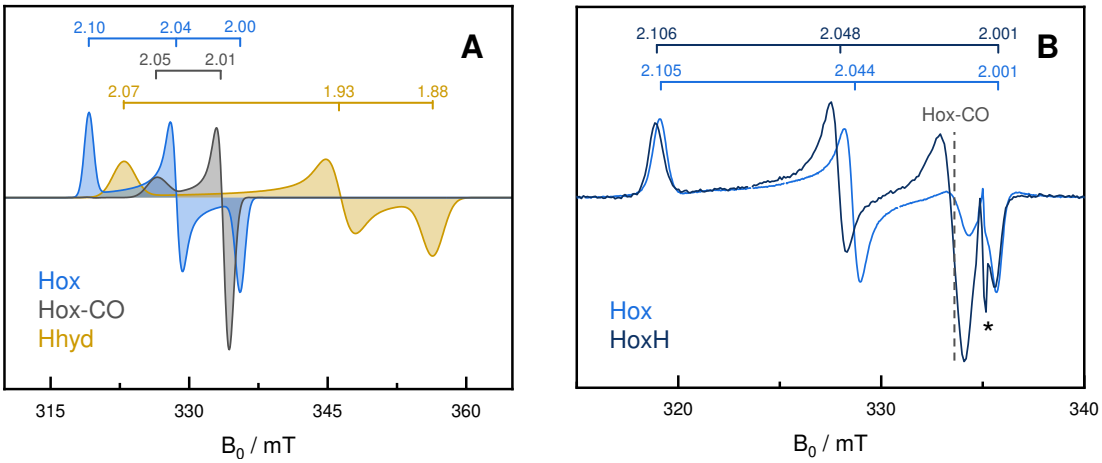

389

390 ***Figure 6 - EPR signatures of the H-cluster in key redox states.*** *All data for CrHydA1.* ***(A)***
391 *Simulations of EPR spectra for the oxidized states* ***Hox*** *and* ***Hox-CO*** *as well as the reduced*
392 *state* ***Hhyd****. The g-values are indicated. The EPR spectrum of* ***Hsred*** *is under debate.* ***(B)***
393 *Experimental EPR spectra of the oxidized state* ***Hox*** *and the oxidized protonated state* ***HoxH***
394 *displaying a subtle shift in g-tensors. Both samples show a contamination with* ***Hox-CO*** *and*
395 *artifacts of the quartz cuvette (*). Experimental conditions: T = 15 K, frequency = 9.4 GHz,*
396 *microwave power = 4 µW, modulation frequency/ amplitude = 100 kHz/ 0.5 mT, and*
397 *conversion time = 60 ms.*

398

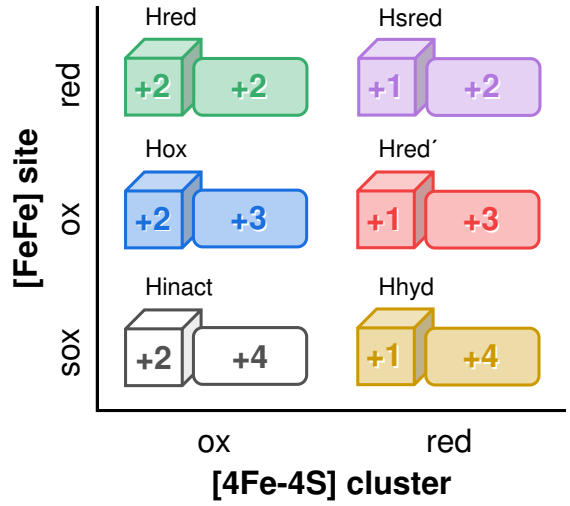

399

400 ***Figure 7 - Electronic properties of key redox states.*** *The [4Fe-4S] cluster is drawn as a cube,*
401 *the diiron site is represented by a rectangular box. The abbreviations refer to either reduced*
402 *(red, Fe_p(I)-Fe_d(I)), oxidized (ox, Fe_p(I)-Fe_d(II)), or super-oxidized (sox, Fe_p(II)-Fe_d(II)) diiron*
403 *site (y-axis) and either reduced (red, +1) or oxidized (ox, +2) [4Fe-4S] cluster (x-axis). The*

*following details are not shown (see text): The electronic configuration of **Hox-CO** and **Hred´-CO** is the same as in **Hox** and **Hred´**, respectively. **Hhyd** binds a terminal hydride, which contributes two additional electrons. Similarly, **Hred** and **Hsred** can be described as with an Fe(II)-Fe(II) site and a bridging hydride. An isoelectronic transition from **Hsred** to **Hhyd** might be possible. **Htrans**, the one-electron reduced form of **Hinact**, would occupy the same position as **Hhyd** in this diagram.*

3.1.2 Vibrational Properties of the H-cluster

The CO and CN^- ligands preserve the low-spin character of the diiron site[115,116] and couple the H-cluster to the protein environment.[50] Making use of FTIR spectroscopy, the CO/CN^- stretching frequencies can be addressed as intrinsic marker bands (Figure 8). They are characteristic for the geometry and the protonation state of all H-cluster intermediates independent of magnetic properties and ^{57}Fe labelling. For example, the **Hox** state shows a clear pattern of five bands that were assigned to uncoupled stretching vibrations of the CO and CN^- ligands at each iron ion and a Fe-Fe bridging carbonyl (μCO) vibration at lower frequencies.[117] Under acidic conditions, the small linear *upshift* of vibrational frequencies in the protonated resting state **HoxH** (mean off-set ~6 cm^{-1} relative to **Hox**) was assigned to a protonation event at the [4Fe-4S] cluster (as discussed above) . Uniform shifts were observed between **Hred´** and **Hred´H**[118], and a recent X-ray free electron laser (XFEL) structure suggests that changes in the orientation of a serine near the [4Fe-4S] cluster (S_2 in Figure 4) may have an effect similar to an adjacent protonation.[53] In contrast, the small linear *downshift* of frequencies in the transition from **Hox** to **Hred´** (mean off-set ~5 cm^{-1}) suggested reduction to the [4Fe-4S] cluster most likely concerted with a protonation event at the same site.[118,119] The hydride state **Hhyd** represents an H-cluster species with most of the electron density located at the Fe_d-H^- bond and the [4Fe-4S] cluster formally rendering the diiron site a super-oxidized Fe(II)-Fe(II) species.[110–113] This results in a mean *upshift* of the CO/CN^- signature by

~20 cm^{-1} relative to **Hox**, which is comparable to **Htrans**.[120] Apparently, the terminal hydride species and the reduced [4Fe-4S] cluster damp the frequency increase expected from the oxidation of the diiron site. In comparison to **Hox/HoxH** and **Hred´/Hred´H**, the irregular shift of frequencies in **HhydH⁺** against **Hhyd** may stem from protonation of the amine headgroup of the adt ligand.[110,121] Other hydride-like H-cluster intermediates (Hhyd:ox and Hyd:red) were identified by laser irradiation of reduced [FeFe]-hydrogenase under cryogenic conditions.[108]

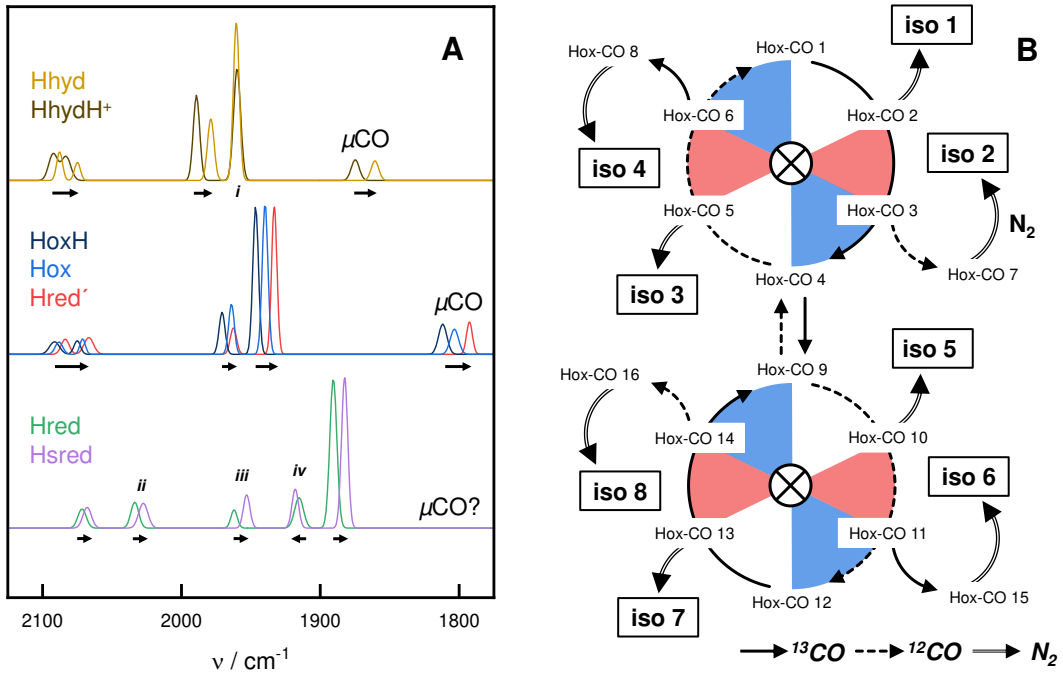

Figure 8 - IR signature of the H-cluster in key redox states and isotope editing. *All data for CrHydA1.* ***(A)*** *Gaussian fits of experimental IR spectra for Fe(II)-Fe(II), Fe(I)-Fe(II), and Fe(I)-Fe(I) species of the H-cluster (top to bottom). Arrows highlight spectral shifts that were assigned to protonation and/or redox differences at the [4Fe-4S] cluster. Note the following irregularities: (i) Relative to* ***Hox/HoxH*** *and* ***Hred´/Hred´H*** *the shift between* ***Hhyd*** *and* ***HhydH⁺*** *is less regular. (ii) One of the* CN^- *ligands is strongly downshifted in* ***Hred*** *and* ***Hsred****. (iii) The conversion of μCO into a terminal CO ligand upon reduction of the diiron site is under discussion. (iv) Note the inversion of band frequencies.* ***(B)*** *Site-selective* ^{13}CO *isotope editing of [FeFe]-hydrogenase under different illumination conditions (white area, dark; red area, 640 nm; blue area, 460 nm). The technique allows accumulation of all 16 CO isotopomers of* ***Hox-CO*** *and all 8 non-inhibited H-cluster states (****Hox****). See ref. 123 for details.*

The vibrations of the CO/CN^- ligands are largely uncoupled in the 'Hox-like' states that are characterized by a μCO geometry and an open coordination site or terminal hydride ligand at the distal iron ion. Other H-cluster states exhibit pronounced vibrational coupling, *e.g.* upon reduction of the diiron site or CO inhibition.[109,117,120] Here, site-selective ^{13}CO isotope editing (Figure 8) in combination with quantum mechanical (QM) calculations allows unraveling the structure of H-cluster intermediates with great precision, *i.e.* simulating the coupling patterns for a given structure with respect to the change in mass.[122] The statistics obtained in such experiments suggested the presence of an apical CN^- ligand in **Hox-CO** and **Hred´-CO**[123,124] hydrogen-bonded to adt-NH in a similar fashion as the apical hydride of **Hhyd**.[89] Moreover, the vibrational energy transfer in **Hred** and **Hsred** at room temperature hints at a cofactor geometry with an apical *d*CO ligand and a Fe-Fe bridging hydride (μH).[125] Cryogenic FTIR, on the other hand, suggested a diverging band pattern for these states (**Chapter 3.3**) incompatible with a μH ligand. Independent of temperature, **Hred** and **Hsred** show a number of further irregularities, *e.g.* the large frequency difference between *p*CN^- and *d*CN^- and the *upshift* of the *p*CO frequency upon reduction of the [4Fe-4S] cluster. The conflicting proposals for the geometry of **Hred** and **Hsred** are discussed in the next chapter.

3.2 Biophysical Investigations *in cristallo*

The crystal structure of the [FeFe]-hydrogenase from *C. pasteurianum* and *D. desulfuricans* by X-ray diffractometry (XRD) laid the foundation for a molecular understanding of hydrogen catalysis.[12,13] Hot on the heels of the oxidized resting state **Hox**, *Cp*I was crystallized in the presence of CO[126–128] and *Dd*H was crystallized in the presence of H_2[129] resulting in H-cluster geometries that served as models for **Hox-CO** and **Hred**, respectively. Even though those crystal structures provide an exceptionally strong starting point for understanding of [FeFe]-hydrogenase chemistry, detailed insight into the dynamic geometry of the H-cluster is dependent on spectroscopy and QM calculations.[130–134] As discussed in the preceding chapter,

alternative ligand orientations in **Hox-CO**, **Hred**, and **Hsred** have been proposed. The limited spatial resolution of XRD on protein crystals impedes a distinction between the diatomic ligands at the H-cluster, which is why CO and CN^- were assigned according to potential hydrogen-bonding contacts with the protein fold in the oxidized state.[12,13] At the proximal iron ion, the original CO/CN^- assignment was found to be correct.[50] But while the crystal structure of CO-inhibited enzyme was modelled with an apical CO ligand (position 'X' in Figure 1),[126–128] vibrational coupling clearly suggested two equatorial carbonyls and an apical CN^- ligand at the distal iron ion in **Hox-CO**.[122–124] This implies pronounced rotational freedom of ligands. Such dynamics are likely to play a role in the reaction with molecular oxygen[135] and the accumulation of the diiron-site reduced states **Hred** and **Hsred**.

The crystal structure of the reduced [FeFe]-hydrogenase *Dd*H showed changes in the electron density of the H-cluster that were interpreted as a 'semi-bridging' CO ligand in a terminal, equatorial position at the distal iron ion.[129] At first glance, this interpretation is supported by room temperature IR spectroscopy as neither *Dd*H nor *Cr*HydA1 show a low frequency peak in the IR signature of **Hred** (compare Figure 8).[120,136] But the vibrational coupling observed in **Hred** and **Hsred** is not compatible with a 'semi-bridging' CO geometry and rather suggests an apical CO ligand.[125] Whether the protection against CO inhibition in these states[89] is related to the reduction of the diiron site or the presence of an apical CO ligand remains to be clarified. Interestingly, cryogenic IR spectroscopy indicated a bridging ligand for both **Hred** and **Hsred**.[108,137,138] This is in agreement with a recent study by Artz *et al.* comparing cryogenic *Cp*I crystal structures solved with both synchrotron radiation and the free electron laser (XFEL) light source at Stanford.[53] The authors were able to quantify the extent of photoreduction suggesting that in the presence of strong reductant up to 50% of *Cp*I was found in a "more reduced conformation" featuring the H-cluster in a μCO geometry.

Outlook. Crystallized in the presence of H_2, the structure of *Dd*H provides insight into the reduced form(s) of the H-cluster.[129] However, a pure accumulation of **Hred** has never been proven *in cristallo* and the coordinates as reported by Nicolet *et al.* in 2001 most likely represent an ensemble of different reduced H-cluster intermediates. To assign XRD structural data, it will be necessary to investigate protein crystals by spectroscopy. In this context, single-crystal EPR spectroscopy is an exceptionally powerful tool for probing paramagnetic intermediates. As nicely exemplified by work on [NiFe]-hydrogenase[139], it provides a method not just for verification of XRD sample status but also generates additional highly detailed experimental insight on electronic and geometric structure of the cofactor. Recent improvements in resonator design enabled its application also on [FeFe]-hydrogenase by Sidabaras *et al.*[140] Unfortunately, EPR spectroscopy is not applicable for all H-cluster states (**Chapter 3.1.1**) creating a need for additional spectroscopic methods. To this end, Ash *et al.* reported a FTIR spectro-electrochemical setup that allows probing single protein crystals by *in situ* IR microscopy as a function of applied potential.[141] The authors could demonstrate how a crystalized [NiFe]-hydrogenase switches from a reduced state (Ni-R) to an oxidized state (Ni-B), and *vice versa*. In the future, similar experiments will facilitate a validation of [FeFe]-hydrogenase redox states formed *in cristallo*, *e.g.* in the process of crystal growth under H_2 or CO. More elegantly, the enzyme could be adjusted to the redox state of interest electrochemically *in situ*, *i.e.* directly ahead of the XRD experiment. Within a relatively narrow time-frame, combining IR absorbance and XRD in a single setup will be feasible.[142] The influence of temperature is discussed in the next chapter.

3.3 The Influence of Temperature

While many techniques demand refrigeration or cryogenic temperatures < 90 K (*e.g.*, synchrotron XRD and XAS/XES, NRVS, Raman, EPR, and Mössbauer spectroscopy) others are compatible with ambient conditions (*e.g.*, FTIR and UV/vis spectroscopy, protein film

electrochemisty, and biochemical analyses). With respect to [FeFe]-hydrogenase, recent results indicate that a direct comparison is not always possible, in particular regarding the geometry of the reduced H-cluster. Making use of FTIR spectro-electrochemistry under ambient conditions, several groups demonstrated the apparent disappearance of the μCO band together with the appearance of a new band in the region associated with terminal CO ligands. This was interpreted as a shift of the μCO ligand into a terminal position upon accumulation of **Hred** and **Hsred**.[120,125,129,136] These findings were supported by investigations on H_2- and/or dithionite-reduced enzyme under ambient conditions, albeit such experiments generally result in a greater variety of redox states (*i.e.*, including **Hhyd**).[89,143] Co-accumulation with **Hred´** complicated the assignment of **Hred** and led to the incorrect conclusion that **Hred** featured a μCO band in *Cr*HydA1.[107] Once **Hred´** had been properly identified[52,118], the absence of a classic μCO ligand in **Hred** and **Hsred** was largely agreed upon. The crystal structure of reduced *Dd*H seemed to support this, as discussed above (**Chapter 3.2**).[129]

Making use of FTIR spectroscopy on H_2- and dithionite-reduced hydrogenase under cryogenic conditions, three recent studies identified low-frequency bands that were not observed at ambient temperatures. For *Dd*H, *Cr*HydA1, and *Ca*I these bands were assigned to a μCO ligand in **Hred** (~1809 ±8 cm^{-1}) and **Hsred** (~1800 ±3 cm^{-1}).[108,137,138] Surprisingly, these μCO frequencies are in the same range as **Hox** and **Hred´** (Figure 8), which would hint at a mixed valence rather than a fully reduced configuration of the diiron site. Under ambient conditions, the μCO stretching frequency is well conserved (Table 1) and has proven to be an excellent reporter of the electron density distribution across the diiron site (**Chapter 3.1.2**), *i.e.* due to his symmetric position between the proximal and distal ion ion. Additionally, the μCO vibration is uncoupled from the terminal CO ligands[52], which allows interrogating the μCO vibration for protonation and redox differences independent of H-cluster geometry. Between Fe(II)-Fe(II) in **Hhyd** and Fe(I)-Fe(II) in **Hox** the difference is ~60 cm^{-1}, for example (Figure

8).[112] In the Group C [FeFe]-hydrogenase from *T. maritima* **Hred** and **Hsred** display a distinct μCO ligand at ambient conditions, which is the reason Chongdar *et al.* introduced the nomenclature Hred* and Hsred*. Here, the μCO frequency difference between Fe(I)-Fe(II) in **Hox** and Fe(I)-Fe(I) in **Hsred** is ~50 cm^{-1}.[35] It should be mentioned that a similar low frequency μCO band has been assigned to the mixed valence diiron site of **Hox** in *Cp*II, a representative of the Group A [FeFe]-hydrogenases (sub-class M2).[53]

Table 1. *Infrared signature of* ***Hox*** *for prototypical Group A [FeFe]-hydrogenases at room temperature. The CO/CN^- frequencies are given in cm^{-1}.*

enzyme	*p*CN	*d*CN	*p*CO	*d*CO	*μ*CO	ref.
*Dd*H	2093	2078	1965	1940	1802	120
*Cr*HydA	2088	2070	1964	1940	1802	107
*Cb*A5H	2091	2080	1964	1940	1800	70
*Me*HydA	2087	2079	1964	1937	1803	66
*Cp*I*	2069	2081	1970	1947	1801	53
*Ca*I*	2070	2082	1970	1947	1802	137

* Due to difference in the active site niche (P-motif), the assignment of *p*CN^- and *d*CN^- has been found to be inverted in *Cp*I and *Ca*I (see ref. 50).

Based on the observation that the terminal CO ligands do not significantly change with temperature, Birrell *et al.* speculate that the μCO ligand in **Hred** and **Hsred** is present under ambient conditions as well, *i.e.* with a reduced absorption coefficient that impedes detection.[138] Arguably, the small frequency differences for the terminal CO ligands upon cooling hint at structural changes in the H-cluster environment, *i.e.* involving residues directly interacting with the cofactor (**Chapter 2.1.2**), rather than independent H-cluster states with a very similar IR signature. However, more detailed studies on the vibrational line broadening as a function of temperature are required. Clarifying the influence of temperature, additional experiments will be necessary, *e.g.* addressing the glass transition from ambient to refrigeration temperatures.

Outlook. Thermodynamic considerations exclude H-cluster intermediates with larger structural differences from the catalytic cycle[130,134,144], which raised the question whether **Hred** and **Hsred** can play a role in the rapid hydrogen turnover of [FeFe]-hydrogenase (**Chapter 4**).[145] Today, ambient and cryogenic measurements show both the presence of an additional terminal CO ligand at room temperature[120,125,129,136] and the presence of a μCO ligand at cryogenic temperature.[108,137,138] Moreover, the geometry of **Hred** and **Hsred** under ambient conditions is hotly debated, with regards to protonation sites and whether the diiron site adopts an H_2-inhibited, μH geometry or an active-ready, 'Hox-like' geometry with a μCO ligand.[125]

In order to understand the interconversion of ambient and cryogenic species of the H-cluster, it will be important to consider the influence of rotational freedom and protein environment as well as proton transfer and proton-coupled electron transport in the accumulation and 'shaping' of redox states as a function of temperature. The lack of compatibility between recent models underscores the inadequate comprehension of hydrogenase catalysis in general.[145] These considerations are of utmost importance when it comes to the interpretation of crystal structures derived from conventional, cryogenic XRD and spectroscopic investigation *in cristallo* (**Chapter 3.2**). Exploiting XFEL radiation to solve the crystal structure of oxidized and reduced [FeFe]-hydrogenase under ambient conditions is an exciting prospect towards a unification of models. Here, it will be important to investigate enzyme with clear preferences for specific redox states, either natural or semi-synthetic [FeFe]-hydrogenases (**Chapter 2**). Moreover, XFELs can be used for serial femtosecond crystallography (SFX) that allows investigating the structure of short-lived, catalytic intermediates.[146–148] As [FeFe]-hydrogenases are not easily activated, we discuss suitable trigger concepts in the next chapter.

3.4 Beyond Steady-state Spectroscopy

Hydrogenases have been characterized by steady-state spectroscopy (**Chapters 3.1**) and XRD (**Chapter 3.2**). In the case of [FeFe]-hydrogenase, various *operando* or *in situ* methods facilitated recording spectral data or activity profiles as a function of electrochemical potential[149–151], gas composition[89] and reactant concentration[52], visible light irradiation,[100,152] and temperature.[137,138] While *in situ* methods typically provide a time resolution between seconds and hours, transient spectroscopy allows following short-lived cofactor intermediates that are difficult to stabilize under steady-state conditions.

UV/vis and IR spectroscopy are well established for the analysis of transient processes in retinal-, porphyrin-, or flavin-binding proteins.[153–155] This is due to advantageous absorption properties (good signal-to-noise) and the ease of handling visible and infrared light. Here, laser sources are exploited to trigger and trace the natural reactivity of the chromoprotein, *i.e.* in a 'flash photolysis' setup comprising separate beams (as opposed to ultrafast 'pump/probe' spectroscopy).[156,157] Hydrogenases lack a dedicated chromophore thus triggering activity is not trivial. To this end, absorption of laser light can be exploited to induce changes in temperature ('T-jump'), pH, or redox potential, the latter in combination with suitable dyes.[158–160] With the development of tunable quantum cascade lasers (QCL), a powerful tabletop infrared light source became available that can be exploited as broadband probing light in a flash photolysis-type set-up.[156]

Transient infrared spectroscopy on hydrogenases was initially demonstrated on [NiFe]-hydrogenase. Greene *et al.* reported the first characterization of the soluble [NiFe]-hydrogenase from *Pyrococcus furiosus* by QCL flash photolysis in the mid-IR.[161] The authors used either NADH or Cd nanorods (DIR, dot-in-rod) as reductant, transferring an electron to the oxidized hydrogenase upon ionization at 355 nm or 405 nm, respectively (Ni-S → Ni-C).[162,163] In a complementary approach, Greene *et al.* addressed the photolability of a catalytic bridging

hydride intermediate (Ni-C → Ni-S) at 530 nm, efficiently exploiting the bimetallic cofactor as 'caged proton'.[164] Theses studies confirmed the kinetic competence of all observed intermediates. In a proof-of-concept study, the first QCL flash photolysis on [FeFe]-hydrogenase was reported by Mirmohades *et al.* in 2016.[165] Here, the authors followed the re-binding of an inhibiting CO molecule to the H-cluster of *Cr*HydA1 after photolysis at 355 nm (**Hox → Hox-CO**) making use of the natural photosensitivity of iron-carbonyl complexes. The kinetics of CO re-binding were confirmed for several organometallic variants of *Cr*HydA1.[89] A photo triggered transition from **Hox** to **Hred** has been reported for *Ca*I adsorbed to Cd-Se nanocrystals,[166] revealing a distinct H/D isotope effect that is related to proton-coupled electron transfer.[48] Proceeding more deeply into the catalytic cycle, Greene *et al.* exploited NADH as reductant to the electron-bifurcating [FeFe]-hydrogenase *Tm*HydABC when activated at 355 nm.[167] The transient accumulation of **Hsred** and **Hred´** (incorrectly assigned to **Hred** in the publication) over **Hox** was found to be compatible with the relatively low turnover frequency of the enzyme (~10 H_2/s).[168] However, whether these states are relevant to the fast hydrogen turnover of Group A [FeFe]-hydrogenases like *Dd*H (>1,000 H_2/s) remained a matter of speculation. Eventually, Sanchez *et al.* demonstrated the use of Cd-doped nanorods[162,163] for the photoreduction of *Cr*HydA1 *via* mediated electron transfer (MET).[169] A great variety of redox states were observed, including **Hred** and **Hsred** as well as **Hred´** and **Hhyd**.

Outlook. As outlined above, numerous states have been identified under steady-state conditions, which inspired the formulation of different mechanistic proposals (**Chapter 4**). Undoubtedly the next step in mechanistic studies is to investigate the transient catalytic proceedings in [FeFe]-hydrogenase at different temperatures and pH conditions. This will facilitate a temporal separation of redox states. Based on the data reported by Sanchez *et al.*[169], all key redox states (**Hred**, **Hred´**, **Hsred**, and **Hhyd**) may participate in catalytic turnover; however, pH titrations under both oxidizing and reducing conditions indicate significant

differences in the steady-state accumulation of redox states.[170] Such difference will have an influence on kinetic parameters. Making use of eosin Y as a photosensitizer facilitates direct electron transfer (DET) to the hydrogenase[48], which may have an effect on the transient kinetics as well. The photoexcitation at ~530 nm allows using light that does not affect the iron-carbonyl bonds of the H-cluster on short time scales. Cross-coupling of hydrogenase molecules to electron relay compounds or redox dyes represents another option to induce DET.[171] An alternative approach would be addressing the 'natural' photosensitivity of certain redox states, *i.e.* as shown by Greene *et al.* for the bridging hydride intermediate of [NiFe]-hydrogenase[164] and Lorent *et al.* for **Hred** and **Hsred** of *Cr*HydA1 at cryogenic temperatures.[108] In the future, it will be exciting to see how these triggering concepts are utilized in transient UV/vis, FTIR, or X-ray spectroscopy as well as SFX diffraction experiments. Figure 9 summarizes the different trigger concepts discussed and suggested in this chapter.

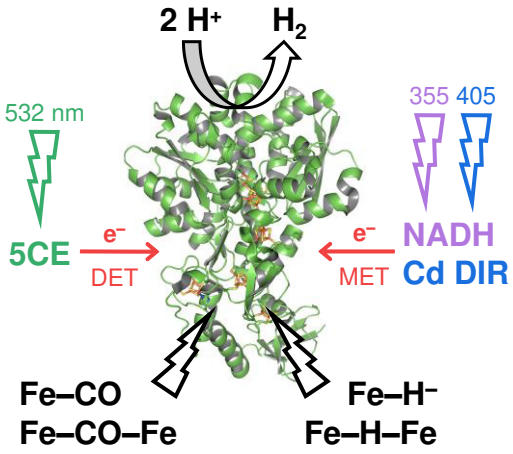

Figure 9 - Triggering hydrogen turnover or catalytic changes by visible light. *NADH and Cd-doped nanorods (dot-in-rod, DIR) were used as redox dyes to follow the transient increase and decrease of several [FeFe]-hydrogenase redox states. In comparison to mediated electron transfer (MET, e.g. using methyl viologen or bipyridinium groups), direct electron transfer (DET) may influence kinetic parameters, e.g. exploiting 5´-carboxy eosin Y (5CE). Addressing the 'natural' photosensitivity of certain redox states represents an alternative approach. Here, iron-carbonyl or iron-hydride bonds are interrogated by visible light of different color.*

3.5 Biophysical Investigations *in vivo*

Mössbauer, EPR, and FTIR spectroscopic measurements with a good signal-to-noise ratio demand purified protein samples, often in high concentration and/or larger quantities. However, the properties of purified hydrogenase may deviate from the enzyme in its native environment, and several aspects of hydrogen turnover were first observed *in vivo*.[23] In 2010, Horch *et al.* reported whole-cell EPR and FTIR spectra of the soluble [NiFe]-hydrogenase from *Ralstonia eutropha* that helped elucidating the mechanism of O_2 tolerance of this particular enzyme.[172] Similar studies on [FeFe]-hydrogenase were not available until 2017 when Berggren *et al.* adopted the protocol of artificial maturation[62,63] to bacterial cells heterologously expressing [FeFe]-hydrogenase apo-protein.[88] This paved the way for the first whole-cell EPR study on *Cr*HydA1 in recombinant *E. coli* cells.[173]

The paramagnetic states **Hox** and **Hox-CO** give relatively unperturbed signals in whole-cell EPR, comparable with purified enzyme (Figure 10).[174] These signatures have been exploited by Land *et al.* to screen uncharacterized [FeFe]-hydrogenases in *E. coli*, circumventing the means of protein purification for preliminary identification and characterization.[36] Moreover, this latter study comprises the first whole-cell FTIR evaluation of [FeFe]-hydrogenase, which proved to be challenging due to low signal intensity in the CO/CN^- frequency regime of the H-cluster and significant overlap with water absorption. Investigating the Group D [FeFe]-hydrogenase *Tam*HydA, for the first time an EPR-silent reduced H-cluster state (*i.e.*, **Hred**) could be identified in a living organism. Cell lysates containing catalytically active [FeFe]-hydrogenases like *Cr*HydA1 and the M2-type [FeFe]-hydrogenase HYDA *from Solobacterium moorei* (M2) even showed a clear current response in chronoamperometric experiments depending on whether H_2 was available for oxidation or not.[36] Recently, Mészáros *et al.* used near-field optimal microscopy (sSNOM) to map the protein content of recombinant *E. coli* cells (Figure 10).[121] No protein was detected outside the cell bodies indicating that all spectroscopic

results stem from hydrogenase inside the bacteria. Varying the redox conditions, pH value, and gas atmosphere, EPR and FTIR spectroscopy verified the formation of reactive hydride states under cellular conditions, including **Hhyd** and **HhydH⁺** (Figure 10). Note that Mulder *et al.* suggested the existence of **HhydH⁺** previously, albeit with an incomplete IR signature.[110]

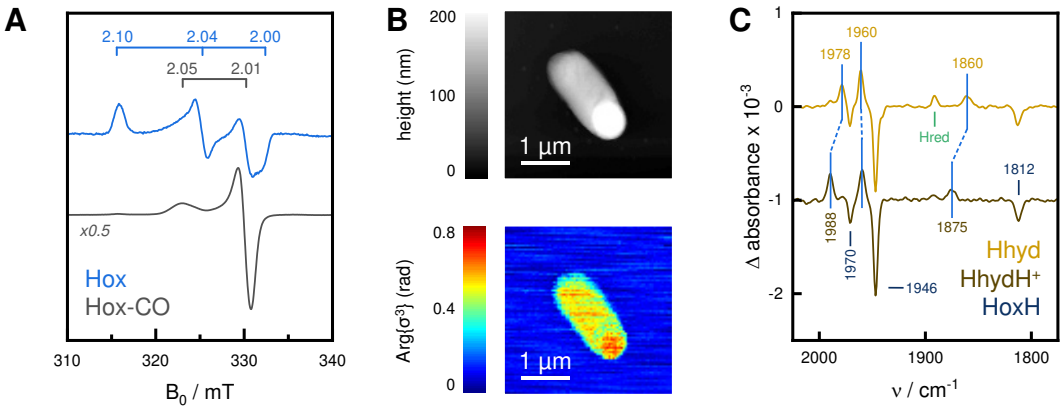

***Figure 10 - Biophysical investigations in vivo**. **(A)** Whole-cell EPR spectra recorded of cells incubated in the absence (upper spectrum) and presence of CO gas (lower spectrum). The signatures of **Hox** and **Hox-CO** are clearly detectable. **(B)** Atomic force microscopy (upper panel) and scattering-type scanning near-field optical microscopy (sSNOM) on recombinant E. coli cells. The sSNOM map was recorded at 1660 cm^{-1}, indicating the lack of protein-specific signal anywhere outside the cell. **(C)** Whole-cell ATR FTIR difference spectroscopy. At low pH and in the presence of H_2, a pattern characteristic of **Hhyd - HoxH** (upper spectrum) was observed. When the concentration of dithionite in the sample was increased, **HhydH⁺** was found to be accumulated over **HoxH** (lower spectrum).*

Outlook. The first generation of whole-cell biophysical investigations agrees with most measurements performed on purified enzyme. Recombinant hydrogenase was found to react surprisingly fast to changes in buffer, redox potential, pH, and gas composition. H-cluster states **Hox**, **Hred**, and **Hhyd** could be detected in living cells, even under mildly alkaline conditions.[121] However, elusive species like **Hred´** and **Hsred** were barely observed. This is indicative of oxidation and docking to the energy metabolism of host cells, *i.e. via* the bacterial

ferredoxin as demonstrated by Barstow *et al.* before.[175] In the future, it will be exciting to study the physiological involvement of hydrogenase in recombinant bacteria and green algae, *e.g.* in the context of bifurcation or photosynthesis.[176–178] Using suitable dyes, fluorescence microscopy could give further insight in pH changes or H_2 release of single cells.[179–181] Methodically, EPR and FTIR spectroscopy proved to be powerful tools for the analysis of recombinant whole cells. It may be possible to optimize the chemical sensitivity and spatial resolution of near-field techniques to reveal the intracellular location of hydrogenase based on the CO/CN^- signature of the H-cluster.[182–185] Film electrochemistry on intact *E. coli* cells suffered from low catalytic currents; however, introducing electron relays in the outer membrane may establish electrophysiological measurements of hydrogenase activity (for comprehensive reviews on bioelectrochemistry, see Armstrong *et al.* and Del Barrio *et al.*[150,186]).

4. The Catalytic Mechanism

In **Chapter 2.1.1**, we suggested grouping the different [FeFe]-hydrogenases based on their phylogenetic relationship (Group A – D) and domain architecture (M1 – M5). Considering the well-conserved nature of the maturation enzymes (HydEFG), all hydrogenases arguably carry the same H-cluster. However, the presence of up to five F-clusters and deviations in the identity of amino acid residues in proton transfer pathway and active site niche brings forth significant differences in catalytic behavior. Additionally, the advances in artificial maturation allowed exploring variations in cofactor composition beyond the scope of nature (**Chapter 2.1.2**). These findings form the basis to which speculations on the catalytic proceedings of hydrogen turnover must obey.

In **Chapter 3.1** we introduced the huge variety of electronic intermediates adopted by the H-cluster. While some of these intermediates are rather well understood (**Hox, Hred´, Hhyd**) others show controversial characteristics (**Hred, Hsred, Hox-CO**). Understanding the latter states, we suggested combining X-ray diffraction with spectroscopic investigations of crystallized enzyme, *e.g.* as grown under H_2 or adjusted to a certain electrical potential (**Chapter 3.2**). Further complicating the situation, recent findings demonstrated the influence of temperature on the geometry of the H-cluster. This raised general concerns regarding the relevance of cryogenic methods in understanding [FeFe]-hydrogenase. In **Chapter 3.3,** we reviewed the key differences between ambient and cryogenic measurements, suggesting diffraction experiments with XFELs as a powerful technique harvesting structural information under ambient conditions. Besides investigating [FeFe]-hydrogenase with transient spectroscopy methods (**Chapter 3.4**), serial femtosecond crystallography at XFEL sources may also provide time-resolved structural information.

Based on the wealth of biochemical, structural, and spectroscopic data, different catalytic cycles have been suggested.[145] These are subject to constant evolution; therefore, we refrain from reviewing any details. Figure 11 depicts a simplified catalytic cycle that shows the two main models. Going from A – E in the direction of H_2 release, both Birrell *et al.* and Ratzloff *et al.* propose the involvement of **Hred** and **Hsred** (5-step model).[137,138] In the first step, **Hred´** is formed by one-electron reduction of **Hox** (A). The charge resides at the [4Fe-4S] cluster. Upon protonation of the adt ligand ($^{+}NH_2$), it is conceivable that the electron tunnels to the diiron site forming **Hred** (B). In a second step of one-electron reduction, **Hred** is converted into **Hsred** (C). Afterwards, the extra proton at the adt ligand migrates to the open binding site of the distal iron ion and forms **Hhyd**, formally oxidizing the diiron site by two electrons (D). Light-induced FTIR difference spectroscopy demonstrated the conversion of **Hred** into Hhyd:ox and **Hsred** into Hhyd:red, which indicates that the formation of **Hhyd** over **Hsred** is

formally allowed.[108] The reduced [4Fe-4S] cluster and hydrogen bonding between adt and Fe_d-H^- stabilizes the super-oxidized diiron site.[89] Upon proton transfer *via* the adt ligand, the terminal hydride combines to H_2, presumably including transient H-cluster states like **HhydH$^+$** and **Hox-H$_2$** (not shown).[108] Eventually, release of H_2 restores the oxidized resting state **Hox** (E).

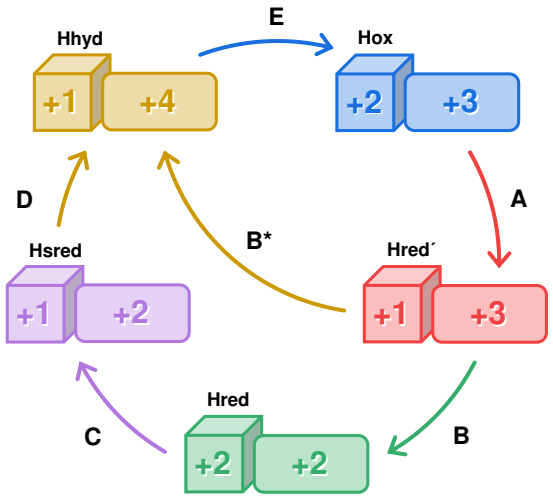

Figure 11 – Possible succession of redox intermediation in biological hydrogen turnover. *The 5-step model (A – E) includes* ***Hred*** *and* ***Hsred****, presuming the H-cluster retains the μCO ligand upon reduction of the diiron site. The 3-step model (A – B* – E) suggests a 'short-cut' from* ***Hred´*** *to* ***Hhyd*** *as both species share the same geometry. The geometry of* ***Hred*** *and* ***Hsred*** *under ambient conditions is debated. See text for details.*

The 5-step model in Figure 11 is based on the interpretation of **Hred** and **Hsred** as H-cluster intermediates with an open coordination site at the distal iron ion, not unlike **Hox** or **Hred´**. As discussed in **Chapter 3.2**, this was concluded from the XRD structure of reduced enzyme, showing a 'semi-bridging' CO ligand and no electron density in the apical position.[129] However, recent FTIR investigation under *cryogenic* conditions by both Birrell *et al.* and Ratzloff *et al.* instead suggest fully-bridged models for **Hred** and **Hsred** (**Chapter 3.3**). Investigating H-cluster reduction under ambient conditions, Mebs *et al.* proposed an alternative

interpretation of the diiron site geometry in **Hred** and **Hsred**.[125] Here, the presence of a apical CO ligand at the distal iron ion alongside stabilization of charge *via* a bridging hydride species puts **Hred** and **Hsred** in the position of 'H_2-inhibited' intermediates.[89] The 3-step model in Figure 11 starts with the conversion of **Hox** into **Hred´**, including reduction of the [4Fe-4S] cluster and protonation of a coordinating cysteine residue (A). In a second proton-coupled electron transfer step, **Hhyd** is formed from **Hred´** directly (B*). Stabilizing the reduced [4Fe-4S] cluster *via* protonation in both species impedes electrons 'leaking' into the diiron site.[52,112,118] Dihydrogen release and restoration of **Hox** is believed to occur in a similar fashion as described above (E).

5. Concluding Remarks

We only just scratched the surface of hydrogenase biodiversity. Moving forward, investigating novel [FeFe]-hydrogenases will help understanding the molecular proceedings of hydrogen turnover. Even less comprehensive is our knowledge about how amino acid patterns shape proton transfer, gas channels, and the dynamic geometry of the H-cluster. While organo-metallic variants are not likely to enhance catalytic efficiency, interfering with nature will facilitate our comprehension of the inner workings of [FeFe]-hydrogenase. Future experiments must facilitate connections between data collected under ambient or cryogenic conditions, on isolated enzyme or whole cells, and in-between species. Critically, steady-state measurements must also be complemented with transient spectroscopy studies and high-level QM calculations to verify the catalytic relevance of identified states. Fortunately, the community is not shy tackling such problems with novel techniques, *e.g.* two-dimensional infrared spectroscopy (2DIR),[187] Fourier-transformed alternating current voltammetry (FTacV)[188], or scattering-type scanning near-field optimal microscopy (sSNOM).[121] More will follow, from the biological, chemical, and physical corners of the community, and it will be exciting to participate in the progress.

6. Acknowledgements

We would like to thank Prof. Dr. David R. Britt and Dr. Guodong Rao who provided the EPR spectra of Hox and HoxH. Furthermore, we are thankful for the critical and constructive feedback during peer review. The work presented in this article is supported by Novo Nordisk Foundation (grant agreement No. NNF19OC0055613 to HL). Further, this project has received funding from the European Research Council under the European Union's Seventh Framework Programme (grant agreement No. 714102 to GB) and Horizon 2020 research and innovation programme (Marie Sklodowska-Curie grant agreement No. 897555 to MS). Additionally, this project was supported by the Deutsche Forschungsgemeinschaft through the priority program 1927 (grant agreement No. 1554/5-1 to STS).

7. References

(1) Marbán, G.; Valdés-Solís, T. Towards the Hydrogen Economy? *Int. J. Hydrogen Energy* **2007**, *32* (12), 1625–1637.

(2) Züttel, A.; Remhof, A.; Borgschulte, A.; Friedrichs, O. Hydrogen: The Future Energy Carrier. *Philos. Trans. R. Soc. A Math. Phys. Eng. Sci.* **2010**, *368* (1923), 3329–3342.

(3) Hosseini, S. E.; Wahid, M. A. Hydrogen Production from Renewable and Sustainable Energy Resources: Promising Green Energy Carrier for Clean Development. *Renew. Sustain. Energy Rev.* **2016**, *57*, 850–866.

(4) Martin, W.; Müller, M. The Hydrogen Hypothesis for the First Eukaryote. *Nature* **1998**, *392*, 37–41.

(5) Lubitz, W.; Ogata, H.; Rüdiger, O.; Reijerse, E. Hydrogenases. *Chem. Rev.* **2014**, *114* (8), 4081–4148.

(6) Madden, C.; Vaughn, M. D.; Díez-Pérez, I.; Brown, K. A.; King, P. W.; Gust, D.; Moore, A. L.; Moore, T. A. Catalytic Turnover of [FeFe]-Hydrogenase Based on Single-Molecule Imaging. *J. Am. Chem. Soc.* **2011**, *143* (3), 1577–1582.

(7) Meyer, J. [FeFe] Hydrogenases and Their Evolution: A Genomic Perspective. *Cell. Mol. Life Sci.* **2007**, *64* (9), 1063–1084.

(8) Calusinska, M.; Happe, T.; Joris, B.; Wilmotte, A. The Surprising Diversity of Clostridial Hydrogenases: A Comparative Genomic Perspective. *Microbiology* **2010**, *156* (6), 1575–1588.

(9) Peters, J. W.; Schut, G. J.; Boyd, E. S.; Mulder, D. W.; Shepard, E. M.; Broderick, J. B.; King, P. W.; Adams, M. W. [FeFe]- and [NiFe]-Hydrogenase Diversity, Mechanism, and Maturation. *Biochim. Biophys. Acta* **2015**, *1853* (6), 1350–1369.

(10) Corr, M. J.; Murphy, J. a. Evolution in the Understanding of [Fe]-Hydrogenase. *Chem. Soc. Rev.* **2011**, *40* (5), 2279–2292.

(11) Benoit, S. L.; Maier, R. J.; Sawers, R. G.; Greening, C. Molecular Hydrogen Metabolism: A Widespread Trait of Pathogenic Bacteria and Protists. *Microbiol. Mol. Biol. Rev.* **2020**, *84* (1), e00092-19.

(12) Peters, J. W.; Lanzilotta, W. N.; Lemon, B. J.; Seefeldt, L. C. X-Ray Crystal Structure of the Fe-Only Hydrogenase (CpI) from Clostridium Pasteurianum to 1.8 Angstrom Resolution. *Science* **1998**, *282* (5395), 1853–1858.

(13) Nicolet, Y.; Piras, C.; Legrand, P.; Hatchikian, C. E.; Fontecilla-Camps, J. C. Desulfovibrio Desulfuricans Iron Hydrogenase: The Structure Shows Unusual Coordination to an Active Site Fe Binuclear Center. *Structure* **1999**, *7* (1), 13–23.

(14) Posewitz, M. C.; King, P. W.; Smolinski, S. L.; Zhang, L.; Seibert, M.; Ghirardi, M. L. Discovery of Two Novel Radical S-Adenosylmethionine Proteins Required for the Assembly of an Active [Fe] Hydrogenase. *J. Biol. Chem.* **2004**, *279* (24), 25711–25720.

(15) King, P. W.; Posewitz, M. C.; Ghirardi, M. L.; Seibert, M. Functional Studies of [FeFe] Hydrogenase Maturation in an Escherichia Coli Biosynthetic System. *J. Bacteriol.* **2006**, *188* (6), 2163.

(16) McGlynn, S. E.; Shepard, E. M.; Winslow, M. a; Naumov, A. V; Duschene, K. S.; Posewitz, M. C.; Broderick, W. E.; Broderick, J. B.; Peters, J. W. HydF as a Scaffold Protein in [FeFe] Hydrogenase H-Cluster Biosynthesis. *FEBS Lett.* **2008**, *582* (15), 2183–2187.

(17) Czech, I.; Silakov, A.; Lubitz, W.; Happe, T. The [FeFe]-Hydrogenase Maturase HydF from Clostridium Acetobutylicum Contains a CO and CN- Ligated Iron Cofactor. *FEBS Lett.* **2010**, *584* (3), 638–642.

(18) Stephenson, M.; Stickland, L. H. Hydrogenase: A Bacterial Enzyme Activating Molecular Hydrogen: The Properties of the Enzyme. *Biochem. J.* **1931**, *25*, 205–214.

(19) Winkler, M.; Esselborn, J.; Happe, T. Molecular Basis of [FeFe]-Hydrogenase Function: An Insight into the Complex Interplay between Protein and Catalytic Cofactor. *Biochim. Biophys. Acta* **2013**, *1827* (8–9), 974–985.

(20) Vignais, P. M.; Billoud, B.; Meyer, J. Classification and Phylogeny of Hydrogenases. *FEMS Microbiol. Rev.* **2001**, *25*, 455–501.

(21) Vignais, P. M.; Billoud, B. Occurrence, Classification, and Biological Function of Hydrogenases: An Overview. *Chem. Rev.* **2007**, *107* (10), 4206–4272.

(22) Greening, C.; Biswas, A.; Carere, C. R.; Jackson, C. J.; Taylor, M. C.; Stott, M. B.; Cook, G. M.; Morales, S. E. Genomic and Metagenomic Surveys of Hydrogenase Distribution Indicate H 2 Is a Widely Utilised Energy Source for Microbial Growth and Survival. *ISME J.* **2016**, *10* (3), 761–777.

(23) Elsden, S. R. Hydrogenase 1931-1981. *Trends Biochem. Sci.* **1981**, *6* (9), 251–253.

(24) Winkler, M.; Hemschemeier, A.; Jacobs, J.; Stripp, S. T.; Happe, T. Multiple Ferredoxin Isoforms in Chlamydomonas Reinhardtii - Their Role under Stress Conditions and Biotechnological Implications. *Eur. J. Cell Biol.* **2010**, *89* (12), 998–

1004.

(25) Zhang, P.; Yuly, J. L.; Lubner, C. E.; Mulder, D. W.; King, P. W.; Peters, J. W.; Beratan, D. N. Electron Bifurcation: Thermodynamics and Kinetics of Two-Electron Brokering in Biological Redox Chemistry. *Acc. Chem. Res.* **2017**, *50* (9), 2410–2417.

(26) Schuchmann, K.; Chowdhury, N. P.; Müller, V. Complex Multimeric [FeFe] Hydrogenases: Biochemistry, Physiology and New Opportunities for the Hydrogen Economy. *Front. Microbiol.* **2018**, *9* (DEC), 1–22.

(27) Peters, J. W.; Miller, A. F.; Jones, A. K.; King, P. W.; Adams, M. W. W. Electron Bifurcation. *Curr. Opin. Chem. Biol.* **2016**, *31*, 146–152.

(28) Buckel, W.; Thauer, R. K. Flavin-Based Electron Bifurcation, A New Mechanism of Biological Energy Coupling. *Chem. Rev.* **2018**, *118* (7), 3862–3886.

(29) Schut, G. J.; Mohamed-Raseek, N.; Tokmina-Lukaszewska, M.; Mulder, D. W.; Nguyen, D. M. N.; Lipscomb, G. L.; Hoben, J. P.; Patterson, A.; Lubner, C. E.; King, P. W.; et al. The Catalytic Mechanism of Electron-Bifurcating Electron Transfer Flavoproteins (ETFs) Involves an Intermediary Complex with NAD. *J. Biol. Chem.* **2019**, *294* (9), 3271–3283.

(30) Chongdar, N.; Pawlak, K.; Rüdiger, O.; Reijerse, E. J.; Rodríguez-Maciá, P.; Lubitz, W.; Birrell, J. A.; Ogata, H. Spectroscopic and Biochemical Insight into an Electron-Bifurcating [FeFe] Hydrogenase. *J. Biol. Inorg. Chem.* **2020**, *25*, 135–149.

(31) Kpebe, A.; Benvenuti, M.; Guendon, C.; Rebai, A.; Fernandez, V.; Le Laz, S.; Etienne, E.; Guigliarelli, B.; García-Molina, G.; de Lacey, A. L.; et al. A New Mechanistic Model for an O2-Protected Electron-Bifurcating Hydrogenase, Hnd from Desulfovibrio Fructosovorans. *Biochim. Biophys. Acta - Bioenerg.* **2018**, *1859* (12), 1302–1312.

(32) Happe, T.; Naber, J. D. Isolation, Characterization and N-Terminal Amino Acid Sequence of Hydrogenase from the Green Alga Chlamydomonas Reinhardtii. *Eur. J. Biochem.* **1993**, *214* (2), 475–481.

(33) Glick, B. R.; Martin, W. G.; Martin, S. M. Purification and Properties of the Periplasmatic Hydrogenase from Desulfovibrio Desulfuricans. *Can. J. Microbiol.* **1980**, *26* (10), 1214–1223.

(34) Nakos, G.; Mortenson, L. Purification and Properties of Hydrogenase, an Iron Sulfur Protein, from Clostridium Pasteurianum W5. *Biochim. Biophys. Acta* **1971**, *227* (10), 576–583.

(35) Chongdar, N.; Birrell, J. A.; Pawlak, K.; Sommer, C.; Reijerse, E. J.; Rüdiger, O.; Lubitz, W.; Ogata, H. Unique Spectroscopic Properties of the H-Cluster in a Putative Sensory [FeFe] Hydrogenase. *J. Am. Chem. Soc.* **2018**, *140* (3), 1057−1068.

(36) Land, H.; Ceccaldi, P.; Mészáros, L. S.; Lorenzi, M.; Redman, H. J.; Senger, M.; Stripp, S. T.; Berggren, G. Discovery of Novel [FeFe]-Hydrogenases for Biocatalytic H2-Production. *Chem. Sci.* **2019**, *10* (43), 9941–9948.

(37) Gauquelin, C.; Baffert, C.; Richaud, P.; Kamionka, E.; Etienne, E.; Guieysse, D.; Girbal, L.; Fourmond, V.; André, I.; Guigliarelli, B.; et al. Roles of the F-Domain in [FeFe] Hydrogenase. *Biochim. Biophys. Acta - Bioenerg.* **2018**, *1859* (2), 69–77.

(38) Caserta, G.; Papini, C.; Adamska-Venkatesh, A.; Pecqueur, L.; Sommer, C.; Reijerse, E.; Lubitz, W.; Gauquelin, C.; Meynial-Salles, I.; Pramanik, D.; et al. Engineering an [FeFe]-Hydrogenase: Do Accessory Clusters Influence O2 Resistance and Catalytic Bias? *J. Am. Chem. Soc.* **2018**, *140* (16), 5516–5526.

(39) Rodríguez-Maciá, P.; Pawlak, K.; Rüdiger, O.; Reijerse, E. J.; Lubitz, W.; Birrell, J. A. Intercluster Redox Coupling Influences Protonation at the H-Cluster in [FeFe] Hydrogenases. *J. Am. Chem. Soc.* **2017**, *139* (42), 15122–15134.

(40) Artz, J. H.; Mulder, D. W.; Ratzloff, M. W.; Lubner, C. E.; Zadvornyy, O. A.; Levan, A. X.; Williams, S. G.; Adams, M. W. W.; Jones, A. K.; King, P. W.; et al. Reduction Potentials of [FeFe]-Hydrogenase Accessory Iron-Sulfur Clusters Provide Insights into the Energetics of Proton Reduction Catalysis. *J. Am. Chem. Soc.* **2017**, *139* (28), 9544–9550.

(41) Cohen, J.; Kim, K.; King, P. W.; Seibert, M.; Schulten, K. Finding Gas Diffusion Pathways in Proteins: Application to O2 and H2 Transport in CpI [FeFe]-Hydrogenase and the Role of Packing Defects. *Structure* **2005**, *13* (9), 1321–1329.

(42) Kubas, A.; Orain, C.; Sancho, D. De; Saujet, L.; Sensi, M.; Gauquelin, C.; Meynial-salles, I.; Soucaille, P.; Bottin, H.; Baffert, C.; et al. Mechanism of O2 Diffusion and Reduction in FeFe Hydrogenases. *Nat. Chem.* **2017**, *9*, 88–95.

(43) Lautier, T.; Ezanno, P.; Baffert, C.; Fourmond, V.; Cournac, L.; Fontecilla-Camps, J. C.; Soucaille, P.; Bertrand, P.; Meynial-Salles, I.; Léger, C. The Quest for a Functional Substrate Access Tunnel in FeFe Hydrogenase. *Faraday Discuss.* **2011**, *148*, 385.

(44) Cornish, A. J.; Gärtner, K.; Yang, H.; Peters, J. W.; Hegg, E. L. Mechanism of Proton Transfer in [FeFe]-Hydrogenase from Clostridium Pasteurianum. *J. Biol. Chem.* **2011**, *19*, 38341–38347.

(45) Morra, S.; Giraudo, A.; Di Nardo, G.; King, P. W.; Gilardi, G.; Valetti, F. Site Saturation Mutagenesis Demonstrates a Central Role for Cysteine 298 as Proton Donor to the Catalytic Site in CaHydA [FeFe]-Hydrogenase. *PLoS One* **2012**, *7* (10), e48400.

(46) Cornish, A. J.; Ginovska, B.; Thelen, A.; Da Silva, J. C. S.; Soares, T. A.; Raugei, S.; Dupuis, M.; Shaw, W. J.; Hegg, E. L. Single-Amino Acid Modifications Reveal Additional Controls on the Proton Pathway of [FeFe]-Hydrogenase. *Biochemistry* **2016**, *55* (22), 3165–3173.

(47) Duan, J.; Senger, M.; Esselborn, J.; Engelbrecht, V.; Wittkamp, F.; Apfel, U.-P.; Hofmann, E.; Stripp, S. T.; Happe, T.; Winkler, M. Crystallographic and Spectroscopic Assignment of the Proton Transfer Pathway in [FeFe]-Hydrogenases. *Nat. Commun.* **2018**, *9*, 4726.

(48) Senger, M.; Eichmann, V.; Laun, K.; Duan, J.; Wittkamp, F.; Knör, G.; Apfel, U.-P.; Happe, T.; Winkler, M.; Heberle, J.; et al. How [FeFe]-Hydrogenase Facilitates Bidirectional Proton Transfer. *J. Am. Chem. Soc.* **2019**, *141* (43), 17394–17403.

(49) Knörzer, P.; Silakov, A.; Foster, C. E.; Armstrong, F. A.; Lubitz, W.; Happe, T. Importance of the Protein Framework for Catalytic Activity of [FeFe]-Hydrogenases. *J. Biol. Chem.* **2012**, *287* (2), 1489–1499.

(50) Lampret, O.; Adamska-Venkatesh, A.; Konegger, H.; Wittkamp, F.; Apfel, U.-P.; Reijerse, E. J.; Lubitz, W.; Rüdiger, O.; Happe, T.; Winkler, M. Interplay between CN

Ligands and the Secondary Coordination Sphere of the H-Cluster in [FeFe]-Hydrogenases. *J. Am. Chem. Soc.* **2017**, *139* (50), 18222–18230.

(51) Kertess, L.; Adamska-Venkatesh, A.; Rodríguez-Maciá, P.; Rüdiger, O.; Lubitz, W.; Happe, T. Influence of the [4Fe-4S] Cluster Coordinating Cysteines on Active Site Maturation and Catalytic Properties of C. Reinhardtii [FeFe]-Hydrogenase. *Chem. Sci.* **2017**, *8* (12), 8127–8137.

(52) Senger, M.; Mebs, S.; Duan, J.; Shulenina, O.; Laun, K.; Kertess, L.; Wittkamp, F.; Apfel, U.-P.; Happe, T.; Winkler, M.; et al. Protonation/Reduction Dynamics at the [4Fe–4S] Cluster of the Hydrogen-Forming Cofactor in [FeFe]-Hydrogenases. *Phys. Chem. Chem. Phys.* **2018**, *20*, 3128–3140.

(53) Artz, J. H.; Zadvornyy, O. A.; Mulder, D. W.; Keable, S. M.; Cohen, A. E.; Ratzloff, M. W.; Williams, S. G.; Ginovska, B.; Kumar, N.; Song, J.; et al. Tuning Catalytic Bias of Hydrogen Gas Producing Hydrogenases. *J. Am. Chem. Soc.* **2020**, *142*, 1227−1235.

(54) Shug, A. L.; Wilson, P. W.; Green, D. E.; Mahler, H. R. The Role of Molybdenum and Flavin in Hydrogenase. *J. Am. Chem. Soc.* **1954**, *76* (12), 3355–3356.

(55) Kaur, J.; Kumar, A.; Kaur, J. Strategies for Optimization of Heterologous Protein Expression in E. Coli: Roadblocks and Reinforcements. *Int. J. Biol. Macromol.* **2017**, *106*, 803–822.

(56) Ahmad, M.; Hirz, M.; Pichler, H.; Schwab, H. Protein Expression in Pichia Pastoris: Recent Achievements and Perspectives for Heterologous Protein Production. *Appl. Microbiol. Biotechnol.* **2014**, *98* (12), 5301–5317.

(57) Akhtar, M. K.; Jones, P. R. Deletion of IscR Stimulates Recombinant Clostridial Fe-Fe Hydrogenase Activity and H2-Accumulation in Escherichia Coli BL21(DE3). *Appl. Microbiol. Biotechnol.* **2008**, *78* (5), 853–862.

(58) Kuchenreuther, J. M.; Grady-Smith, C. S.; Bingham, A. S.; George, S. J.; Cramer, S. P.; Swartz, J. R. High-Yield Expression of Heterologous [FeFe] Hydrogenases in Escherichia Coli. *PLoS One* **2010**, *5* (11).

(59) Girbal, L.; Von Abendroth, G.; Winkler, M.; Benton, P.; Meynial-Salles, I.; Croux, C.; Peters, J. W.; Happe, T.; Soucaille, P. Homologous and Heterologous Overexpression in Clostridium Acetobutylicum and Characterization of Purified Clostridial and Algal Fe-Only Hydrogenases with High Specific Activities. *Appl. Environ. Microbiol.* **2005**, *71* (5), 2777–2781.

(60) von Abendroth, G.; Stripp, S. T.; Silakov, A.; Croux, C.; Soucaille, P.; Girbal, L.; Happe, T. Optimized Over-Expression of [FeFe] Hydrogenases with High Specific Activity in Clostridium Acetobutylicum. *Int. J. Hydrogen Energy* **2008**, *33* (21), 6076–6081.

(61) Sybirna, K.; Antoine, T.; Lindberg, P.; Fourmond, V.; Rousset, M.; Méjean, V.; Bottin, H. Shewanella Oneidensis: A New and Efficient System for Expression and Maturation of Heterologous [Fe-Fe] Hydrogenase from Chlamydomonas Reinhardtii. *BMC Biotechnol.* **2008**, *8*, 73.

(62) Berggren, G.; Adamska-Venkatesh, A.; Lambertz, C.; Simmons, T. R.; Esselborn, J.; Atta, M.; Gambarelli, S.; Mouesca, J.-M.; Reijerse, E. J.; Lubitz, W.; et al. Biomimetic

Assembly and Activation of [FeFe]-Hydrogenases. *Nature* **2013**, *499* (7456), 66–69.

(63) Esselborn, J.; Lambertz, C.; Adamska-Venkatesh, A.; Simmons, T.; Berggren, G.; Noth, J.; Siebel, J. F.; Hemschemeier, A.; Artero, V.; Reijerse, E.; et al. Spontaneous Activation of [FeFe]-Hydrogenases by an Inorganic [2Fe] Active Site Mimic. *Nat. Chem. Biol.* **2013**, *9*, 607–609.

(64) Bornscheuer, U. T.; Huisman, G. W.; Kazlauskas, R. J.; Lutz, S.; Moore, J. C.; Robins, K. Engineering the Third Wave of Biocatalysis. *Nature* **2012**, *485* (7397), 185–194.

(65) Hatchikian, E. C.; Forget, N.; Fernandez, V. M.; Williams, R.; Cammack, R. Further Characterization of the [Fe]-Hydrogenase from Desulfovibrio Desulfuricans ATCC 7757. *Eur. J. Biochem.* **1992**, *209* (1), 357–365.

(66) Caserta, G.; Adamska-Venkatesh, A.; Pecqueur, L.; Atta, M.; Artero, V.; Roy, S.; Reijerse, E.; Lubitz, W.; Fontecave, M. Chemical Assembly of Multiple Metal Cofactors: The Heterologously Expressed Multidomain [FeFe]-Hydrogenase from Megasphaera Elsdenii. *Biochim. Biophys. Acta - Bioenerg.* **2016**, *1857* (11), 1734–1740.

(67) Engelbrecht, V.; Rodríguez-Maciá, P.; Esselborn, J.; Sawyer, A.; Hemschemeier, A.; Rüdiger, O.; Lubitz, W.; Winkler, M.; Happe, T. The Structurally Unique Photosynthetic Chlorella Variabilis NC64A Hydrogenase Does Not Interact with Plant-Type Ferredoxins. *Biochim. Biophys. Acta - Bioenerg.* **2017**, *1858* (9), 771–778.

(68) Morra, S.; Maurelli, S.; Chiesa, M.; Mulder, D. W.; Ratzloff, M. W.; Giamello, E.; King, P. W.; Gilardi, G.; Valetti, F. The Effect of a C298D Mutation in CaHydA [FeFe]-Hydrogenase: Insights into the Protein-Metal Cluster Interaction by EPR and FTIR Spectroscopic Investigation. *Biochim. Biophys. Acta - Bioenerg.* **2016**, *1857* (1), 98–106.

(69) Rodríguez-Maciá, P.; Kertess, L.; Burnik, J.; Birrell, J. A.; Hofmann, E.; Lubitz, W.; Happe, T.; Rüdiger, O. His-Ligation to the [4Fe-4S] Subcluster Tunes the Catalytic Bias of [FeFe] Hydrogenase. *J. Am. Chem. Soc.* **2019**, *141* (1), 472–481.

(70) Morra, S.; Arizzi, M.; Valetti, F.; Gilardi, G. Oxygen Stability in the New [FeFe]-Hydrogenase from Clostridium Beijerinckii SM10 (CbA5H). *Biochemistry* **2016**, *55* (42), 5897–5900.

(71) Mulder, D. W.; Ortillo, D. O.; Gardenghi, D. J.; Naumov, A. V.; Ruebush, S. S.; Szilagyi, R. K.; Huynh, B.; Broderick, J. B.; Peters, J. W. Activation of HydA(DeltaEFG) Requires a Preformed [4Fe-4S] Cluster. *Biochemistry* **2009**, *48*, 6240–6248.

(72) Mulder, D. W.; Boyd, E. S.; Sarma, R.; Lange, R. K.; Endrizzi, J. A.; Broderick, J. B.; Peters, J. W. Stepwise [FeFe]-Hydrogenase H-Cluster Assembly Revealed in the Structure of HydA(DeltaEFG). *Nature* **2010**, *465* (7295), 248–251.

(73) Caserta, G.; Pecqueur, L.; Adamska-Venkatesh, A.; Papini, C.; Roy, S.; Artero, V.; Atta, M.; Reijerse, E.; Lubitz, W.; Fontecave, M. Structural and Functional Characterization of the Hydrogenase-Maturation HydF Protein. *Nat. Chem. Biol.* **2017**, *13* (7), 779–784.

(74) Rao, G.; Pattenaude, S. A.; Alwan, K.; Blackburn, N. J.; Britt, R. D.; Rauchfuss, T. B. The Binuclear Cluster of [FeFe] Hydrogenase Is Formed with Sulfur Donated by

Cysteine of an [Fe(Cys)(CO)2(CN)] Organometallic Precursor. *Proc. Natl. Acad. Sci. U. S. A.* **2019**, *116* (42), 20850–20855.

(75) Németh, B.; Esmieu, C.; Redman, H. J.; Berggren, G. Monitoring H-Cluster Assembly Using a Semi-Synthetic HydF Protein. *Dalt. Trans.* **2019**, *48* (18), 5978–5986.

(76) Gilbert-Wilson, R.; Siebel, J. F.; Adamska-Venkatesh, A.; Pham, C. C.; Reijerse, E.; Wang, H.; Cramer, S. P.; Lubitz, W.; Rauchfuss, T. B. Spectroscopic Investigations of [FeFe] Hydrogenase Maturated with [57Fe2(Adt)(CN)2(CO)4]2-. *J. Am. Chem. Soc.* **2015**, *137* (28), 8998–9005.

(77) Adamska-Venkatesh, A.; Simmons, T. R.; Siebel, J. F.; Artero, V.; Fontecave, M.; Lubitz, W. Chlamydomonas Reinhardtii: HYSCORE and ENDOR Study of a Non-Natural H-Cluster. *Phys. Chem. Chem. Phys.* **2015**, *17*, 5421–5430.

(78) Adamska-Venkatesh, A.; Roy, S.; Siebel, J. F.; Simmons, T. R.; Fontecave, M.; Artero, V.; Reijerse, E.; Lubitz, W. Spectroscopic Characterization of the Bridging Amine in the Active Site of [FeFe] Hydrogenase Using Isotopologues of the H-Cluster. *J. Am. Chem. Soc.* **2015**, *137* (40), 12744–12747.

(79) Artero, V.; Berggren, G.; Atta, M.; Caserta, G.; Roy, S.; Pecqueur, L.; Fontecave, M. From Enzyme Maturation to Synthetic Chemistry: The Case of Hydrogenases. *Acc. Chem. Res.* **2015**, *48* (8), 2380–2387.

(80) Birrell, J. A.; Rüdiger, O.; Reijerse, E. J.; Lubitz, W. Semisynthetic Hydrogenases Propel Biological Energy Research into a New Era. *Joule* **2017**, *1* (1), 61–76.

(81) Wittkamp, F.; Senger, M.; Stripp, S. T.; Apfel, U.-P. [FeFe]-Hydrogenases: Recent Developments and Future Perspectives. *Chem. Commun.* **2018**, *54*, 5934–5942.

(82) Esmieu, C.; Raleiras, P.; Berggren, G. From Protein Engineering to Artificial Enzymes-Biological and Biomimetic Approaches towards Sustainable Hydrogen Production. *Sustain. Energy Fuels* **2018**, *2* (4), 724–750.

(83) Sommer, C.; Richers, C. P.; Lubitz, W.; Rauchfuss, T. B.; Reijerse, E. J. A [RuRu] Analogue of an [FeFe]-Hydrogenase Traps the Key Hydride Intermediate of the Catalytic Cycle Angewandte. *Angew. Chemie Int. Ed.* **2018**, *57*, 5429 –5432.

(84) Noth, J.; Esselborn, J.; Güldenhaupt, J.; Brünje, A.; Sawyer, A.; Apfel, U.-P.; Gerwert, K.; Hofmann, E.; Winkler, M.; Happe, T. [FeFe]-Hydrogenase with Chalcogenide Substitutions at the H-Cluster Maintains Full H2 Evolution Activity. *Angew. Chemie Int. Ed.* **2016**, *55*, 8396–8400.

(85) Kertess, L.; Wittkamp, F.; Sommer, C.; Esselborn, J.; Rüdiger, O.; Reijerse, E.; Hofmann, E.; Lubitz, W.; Winkler, M.; Happe, T.; et al. Chalcogenide Substitution in the [2Fe]-Cluster of [FeFe]-Hydrogenases Conserves High Enzymatic Activity. *Dalt. Trans.* **2017**, *46*, 16947–16958.

(86) Siebel, J. F.; Adamska-Venkatesh, A.; Weber, K.; Rumpel, S.; Reijerse, E.; Lubitz, W. Hybrid [FeFe]-Hydrogenases with Modified Active Sites Show Remarkable Residual Enzymatic Activity. *Biochemistry* **2015**, *54* (7), 1474–1483.

(87) Esselborn, J.; Muraki, N.; Klein, K.; Engelbrecht, V.; Metzler-Nolte, N.; Apfel, U.-P.; Hofmann, E.; Kurisu, G.; Happe, T. A Structural View of Synthetic Cofactor Integration into [FeFe]-Hydrogenases. *Chem. Sci.* **2016**, *7*, 959–968.

(88) Khanna, N.; Esmieu, C.; Mészáros, L. S.; Lindblad, P.; Berggren, G. In Vivo Activation of an [FeFe] Hydrogenase Using Synthetic Cofactors. *Energy Environ. Sci.* **2017**, *10* (7), 1563–1567.

(89) Duan, J.; Mebs, S.; Laun, K.; Wittkamp, F.; Heberle, J.; Hofmann, E.; Apfel, U.-P.; Winkler, M.; Senger, M.; Haumann, M.; et al. Geometry of the Catalytic Active Site in [FeFe]-Hydrogenase Is Determined by Hydrogen Bonding and Proton Transfer. *ACS Catal.* **2019**, *9*, 9140–9149.

(90) Tard, C.; Pickett, C. J. Structural and Functional Analogues of the Active Sites of the [Fe]-, [NiFe]-, and [FeFe]-Hydrogenases. *Chem. Rev.* **2009**, *109* (6), 2245–2274.

(91) Simmons, T. R.; Berggren, G.; Bacchi, M.; Fontecave, M.; Artero, V. Mimicking Hydrogenases: From Biomimetics to Artificial Enzymes. *Coord. Chem. Rev.* **2014**, *270–271* (1), 127–150.

(92) Schilter, D.; Camara, J. M.; Huynh, M. T.; Hammes-Schiffer, S.; Rauchfuss, T. B. Hydrogenase Enzymes and Their Synthetic Models: The Role of Metal Hydrides. *Chem. Rev.* **2016**, *116* (15), 8693–8749.

(93) Camara, J. M.; Rauchfuss, T. B. Combining Acid–Base, Redox and Substrate Binding Functionalities to Give a Complete Model for the [FeFe]-Hydrogenase. *Nat. Chem.* **2012**, *4* (1), 26–30.

(94) Ginovska-Pangovska, B.; Dutta, A.; Reback, M. L.; Linehan, J. C.; Shaw, W. J. Beyond the Active Site: The Impact of the Outer Coordination Sphere on Electrocatalysts for Hydrogen Production and Oxidation. *Acc. Chem. Res.* **2014**, *47* (8), 2621–2630.

(95) Plumeré, N.; Rüdiger, O.; Oughli, A. A.; Williams, R.; Vivekananthan, J.; Pöller, S.; Schuhmann, W.; Lubitz, W. A Redox Hydrogel Protects Hydrogenase from High-Potential Deactivation and Oxygen Damage. *Nat. Chem.* **2014**, *6* (9), 822–827.

(96) Oughli, A. A.; Conzuelo, F.; Winkler, M.; Happe, T.; Lubitz, W.; Schuhmann, W.; Rüdiger, O.; Plumerø, N. A Redox Hydrogel Protects the O2-Sensitive [FeFe] - Hydrogenase from Chlamydomonas Reinhardtii from Oxidative Damage. *Angew. Chemie - Int. Ed.* **2015**, *54* (42), 12329–12333.

(97) Ruff, A.; Conzuelo, F.; Schuhmann, W. Bioelectrocatalysis as the Basis for the Design of Enzyme-Based Biofuel Cells and Semi-Artificial Biophotoelectrodes. *Nat. Catal.* **2019**, *3*, 214–224.

(98) Pereira, A. S. S.; Tavares, P.; Moura, I.; Moura, J. J. G. J.; Huynh, B. H. H. Mössbauer Characterization of the Iron-Sulfur Clusters in Desulfovibrio v Ulgaris Hydrogenase. *J. Am. Chem. Soc.* **2001**, *123* (12), 2771–2782.

(99) Schwab, D. E.; Tard, C.; Brecht, E.; Peters, J. W.; Pickett, C. J.; Szilagyi, R. K. On the Electronic Structure of the Hydrogenase H-Cluster. *Chem. Commun.* **2006**, No. 35, 3696–3698.

(100) Sensi, M.; Baffert, C.; Fradale, L.; Gauquelin, C.; Soucaille, P.; Meynial-Salles, I.; Bottin, H.; De Gioia, L.; Bruschi, M.; Fourmond, V.; et al. Photoinhibition of FeFe Hydrogenase. *ACS Catal.* **2017**, *7* (10), 7378–7387.

(101) Lubitz, W.; Reijerse, E.; van Gastel, M. [NiFe] and [FeFe] Hydrogenases Studied by Advanced Magnetic Resonance Techniques. *Chem. Rev.* **2007**, *107* (10), 4331–4365.

(102) Telser, J.; Benecky, M. J.; Adams, M. W. W.; Mortenson, L. E.; Hoffman, B. M. An EPR and Electron Nuclear Double Resonance Investigation of Carbon Monoxide Binding to Hydrogenase I (Bidirectional) from Clostridium Pasteurianum W5. *J. Biol. Chem.* **1986**, *261* (29), 13536–13541.

(103) Telser, J.; Benecky, M. J.; Adams, M. W.; Mortenson, L. E.; Hoffman, B. M. EPR and Electron Nuclear Double Resonance Investigation of Oxidized Hydrogenase II (Uptake) from Clostridium Pasteurianum W5. Effects of Carbon Monoxide Binding. *J. Biol. Chem.* **1987**, *262* (14), 6589–6594.

(104) Reijerse, E.; Birrell, J. A.; Lubitz, W. Spin Polarization Reveals the Coordination Geometry of the [FeFe] Hydrogenase Active Site in Its CO Inhibited State. *J. Phys. Chem. Lett.* **2020**, in press.

(105) Silakov, A.; Wenk, B.; Reijerse, E.; Lubitz, W. 14N HYSCORE Investigation of the H-Cluster of [FeFe] Hydrogenase: Evidence for a Nitrogen in the Dithiol Bridge. *Phys. Chem. Chem. Phys.* **2009**, *11* (31), 6553–6554.

(106) Albracht, S. P. J.; Roseboom, W.; Hatchikian, E. C. The Active Site of the [FeFe]-Hydrogenase from Desulfovibrio Desulfuricans. I. Light Sensitivity and Magnetic Hyperfine Interactions as Observed by Electron Paramagnetic Resonance. *J. Biol. Inorg. Chem.* **2006**, *11* (1), 88–101.

(107) Adamska-Venkatesh, A.; Silakov, A.; Lambertz, C.; Rüdiger, O.; Happe, T.; Reijerse, E.; Lubitz, W. Identification and Characterization of the "Super-Reduced" State of the H-Cluster in [FeFe] Hydrogenase: A New Building Block for the Catalytic Cycle? *Angew. Chemie Int. Ed.* **2012**, *51* (46), 11458–11462.

(108) Lorent, C.; Katz, S.; Duan, J.; Julia Kulka, C.; Caserta, G.; Teutloff, C.; Yadav, S.; Apfel, U.-P.; Winkler, M.; Happe, T.; et al. Shedding Light on Proton and Electron Dynamics in [FeFe] Hydrogenases. *J. Am. Chem. Soc.* **2020**, *142* (12), 5493–5497.

(109) Adamska-Venkatesh, A.; Krawietz, D.; Siebel, J. F.; Weber, K.; Happe, T.; Reijerse, E.; Lubitz, W. New Redox States Observed in [FeFe] Hydrogenases Reveal Redox Coupling within the H-Cluster. *J. Am. Chem. Soc.* **2014**, *136* (32), 11339–11346.

(110) Mulder, D. W.; Ratzloff, M. W.; Bruschi, M.; Greco, C.; Koonce, E.; Peters, J. W.; King, P. W. Investigations on the Role of Proton-Coupled Electron Transfer in Hydrogen Activation by [FeFe]-Hydrogenase. *J. Am. Chem. Soc.* **2014**, *136* (43), 15394–15402.

(111) Mulder, D. W.; Guo, Y.; Ratzloff, M. W.; King, P. W. Identification of a Catalytic Iron-Hydride at the H-Cluster of [FeFe]-Hydrogenase. *J. Am. Chem. Soc.* **2016**, *139* (1), 83–86.

(112) Winkler, M.; Senger, M.; Duan, J.; Esselborn, J.; Wittkamp, F.; Hofmann, E.; Apfel, U.-P.; Stripp, S. T.; Happe, T. Accumulating the Hydride State in the Catalytic Cycle of [FeFe]-Hydrogenases. *Nat. Commun.* **2017**, *8* (16115), 1–7.

(113) Reijerse, E. J.; Pham, C. C.; Pelmenschikov, V.; Gilbert-wilson, R.; Adamska-Venkatesh, A.; Siebel, J. F.; Gee, L. B.; Yoda, Y.; Tamasaku, K.; Lubitz, W.; et al. Direct Observation of an Iron-Bound Terminal Hydride in [FeFe]- Hydrogenase by Nuclear Resonance Vibrational Spectroscopy. *J. Am. Chem. Soc.* **2017**, *139* (12), 4306–4309.

(114) Rumpel, S.; Sommer, C.; Reijerse, E.; Farès, C.; Lubitz, W. Direct Detection of the Terminal Hydride Intermediate in [FeFe] Hydrogenase by NMR Spectroscopy. *J. Am. Chem. Soc.* **2018**, *140* (11), 3863–3866.

(115) Pierik, A. J.; Hulstein, M.; Hagen, W. R.; Albracht, S. P. A Low-Spin Iron with CN and CO as Intrinsic Ligands Forms the Core of the Active Site in [Fe]-Hydrogenases. *Eur. J. Biochem.* **1998**, *258* (2), 572–578.

(116) Pierik, A. J.; Roseboom, W.; Happe, R. P.; Bagley, K. A.; Albracht, S. P. J. Carbon Monoxide and Cyanide as Intrinsic Ligands to Iron in the Active Site of [NiFe]-Hydrogenases. *J. Biol. Chem.* **1999**, *274* (6), 3331–3337.

(117) De Lacey, A. L.; Stadler, C.; Cavazza, C.; Hatchikian, E. C.; Fernandez, V. M. FTIR Characterization of the Active Site of the Fe-Hydrogenase from Desulfovibrio Desulfuricans. *J. Am. Chem. Soc.* **2000**, *122* (45), 11232–11233.

(118) Senger, M.; Laun, K.; Wittkamp, F.; Duan, J.; Haumann, M.; Happe, T.; Winkler, M.; Apfel, U.-P.; Stripp, S. T. Proton-Coupled Reduction of the Catalytic [4Fe-4S] Cluster in [FeFe]-Hydrogenases. *Angew. Chemie Int. Ed.* **2017**, *56* (52), 16503–16506.

(119) Katz, S.; Noth, J.; Horch, M.; Shafaat, H. S.; Happe, T.; Hildebrandt, P.; Zebger, I. Vibrational Spectroscopy Reveals the Initial Steps of Biological Hydrogen Evolution. *Chem. Sci.* **2016**, *7*, 6746–6752.

(120) Roseboom, W.; De Lacey, A. L.; Fernandez, V. M.; Hatchikian, E. C.; Albracht, S. P. J. The Active Site of the [FeFe]-Hydrogenase from Desulfovibrio Desulfuricans. II. Redox Properties, Light Sensitivity and CO-Ligand Exchange as Observed by Infrared Spectroscopy. *J. Biol. Inorg. Chem.* **2006**, *11* (1), 102–118.

(121) Mészáros, L.; Ceccaldi, P.; Lorenzi, M.; Redman, H. J.; Pfitzner, E.; Heberle, J.; Senger, M.; Stripp, S. T.; Berggren, G. Spectroscopic Investigations under Whole Cell Conditions Provide New Insight into the Metal Hydride Chemistry of [FeFe]-Hydrogenase. *Chem. Sci.* **2020**, *11* (18), 4608–4617.

(122) Zilberman, S.; Stiefel, E. I.; Cohen, M. H.; Car, R. Resolving the CO / CN Ligand Arrangement in CO-Inactivated [FeFe] Hydrogenase by First Principles Density Functional Theory Calculations. *Inorg. Chem.* **2006**, *45* (15), 5715–5717.

(123) Senger, M.; Mebs, S.; Duan, J.; Wittkamp, F.; Apfel, U.-P.; Heberle, J.; Haumann, M.; Stripp, S. T. Stepwise Isotope Editing of [FeFe]-Hydrogenases Exposes Cofactor Dynamics. *Proc. Natl. Acad. Sci. U. S. A.* **2016**, *113* (30), 8454–8459.

(124) Laun, K.; Mebs, S.; Duan, J.; Wittkamp, F.; Apfel, U.-P.; Happe, T.; Winkler, M.; Haumann, M.; Stripp, S. T. Spectroscopical Investigations on the Redox Chemistry of [FeFe]-Hydrogenases in the Presence of Carbon Monoxide. *MOLECULES* **2018**, *23* (7), 1669.

(125) Mebs, S.; Senger, M.; Duan, J.; Wittkamp, F.; Apfel, U.-P.; Happe, T.; Winkler, M.; Stripp, S. T.; Haumann, M. Bridging Hydride at Reduced H-Cluster Species in [FeFe]-Hydrogenases Revealed by Infrared Spectroscopy, Isotope Editing, and Quantum Chemistry. *J. Am. Chem. Soc.* **2017**, *139* (35), 12157–12160.

(126) Lemon, B. J.; Peters, J. W. Binding of Exogenously Added Carbon Monoxide at the Active Site of the Iron-Only Hydrogenase (CpI) from Clostridium Pasteurianum. *Biochemistry* **1999**, *38* (40), 12969–12973.

(127) Bennett, B.; Lemon, B. J.; Peters, J. W. Reversible Carbon Monoxide Binding and Inhibition at the Active Site of the Fe-Only Hydrogenase. *Biochemistry* **2000**, *39* (25), 7455–7460.

(128) Lemon, B. J.; Peters, J. W. Photochemistry at the Active Site of the Carbon Monoxide Inhibited Form of the Iron-Only Hydrogenase (CpI). *J. Am. Chem. Soc.* **2000**, *122* (15), 3793–3794.

(129) Nicolet, Y.; De Lacey, A. L.; Vernède, X.; Fernandez, V. M.; Hatchikian, E. C.; Fontecilla-Camps, J. C. Crystallographic and FTIR Spectroscopic Evidence of Changes in Fe Coordination upon Reduction of the Active Site of the Fe-Only Hydrogenase from Desulfovibrio Desulfuricans. *J. Am. Chem. Soc.* **2001**, *123* (8), 1596–1601.

(130) Bruschi, M.; Greco, C.; Kaukonen, M.; Fantucci, P.; Ryde, U.; De Gioia, L. Influence of the [2Fe]H Subcluster Environment on the Properties of Key Intermediates in the Catalytic Cycle of [FeFe] Hydrogenases: Hints for the Rational Design of Synthetic Catalysts. *Angew. Chemie Int. Ed.* **2009**, *48* (19), 3503–3506.

(131) Finkelmann, A. R.; Stiebritz, M. T.; Reiher, M. Inaccessibility of the μ-Hydride Species in [FeFe] Hydrogenases. *Chem. Sci.* **2014**, *5* (1), 215–221.

(132) Blomberg, M. R. a; Borowski, T.; Himo, F.; Liao, R.-Z.; Siegbahn, P. E. M. Quantum Chemical Studies of Mechanisms for Metalloenzymes. *Chem. Rev.* **2014**, *114*, 3601–3658.

(133) Greco, C.; Fourmond, V.; Baffert, C.; Wang, P.; Dementin, S.; Bertrand, P.; Bruschi, M.; Blumberger, J.; De Gioia, L.; Léger, C. Combining Experimental and Theoretical Methods to Learn about the Reactivity of Gas-Processing Metalloenzymes. *Energy Environ. Sci.* **2014**, *7*, 3543–3573.

(134) Filippi, G.; Arrigoni, F.; Bertini, L.; De Gioia, L.; Zampella, G. DFT Dissection of the Reduction Step in H2 Catalytic Production by [FeFe]-Hydrogenase-Inspired Models: Can the Bridging Hydride Become More Reactive Than the Terminal Isomer? *Inorg. Chem.* **2015**, *54* (19), 9529–9542.

(135) Fourmond, V.; Greco, C.; Sybirna, K.; Baffert, C.; Wang, P.-H.; Ezanno, P.; Montefiori, M.; Bruschi, M.; Meynial-Salles, I.; Soucaille, P.; et al. The Oxidative Inactivation of FeFe Hydrogenase Reveals the Flexibility of the H-Cluster. *Nat. Chem.* **2014**, *6* (4), 336–342.

(136) Sommer, C.; Adamska-Venkatesh, A.; Pawlak, K.; Birrell, J. A.; Rüdiger, O.; Reijerse, E. J.; Lubitz, W. Proton Coupled Electronic Rearrangement within the H-Cluster as an Essential Step in the Catalytic Cycle of [FeFe] Hydrogenases. *J. Am. Chem. Soc.* **2017**, *139* (4), 1440−1443.

(137) Ratzloff, M. W.; Artz, J. H.; Mulder, D. W.; Collins, R. T.; Furtak, T. E.; King, P. W. CO-Bridged H-Cluster Intermediates in the Catalytic Mechanism of [FeFe]-Hydrogenase CaI. *J. Am. Chem. Soc.* **2018**, *140* (24), 7623–7628.

(138) Birrell, J. A.; Pelmenschikov, V.; Mishra, N.; Wang, H.; Yoda, Y.; Rauchfuss, T. B.; Cramer, S. P.; Lubitz, W.; Debeer, S. Spectroscopic and Computational Evidence That [FeFe] Hydrogenases Operate Exclusively with CO-Bridged Intermediates Spectroscopic and Computational Evidence That [FeFe] Hydrogenases Operate Exclusively with CO-Bridged. *J. Am. Chem. Soc.* **2020**, *142* (1), 222–232.

(139) Foerster, S.; Stein, M.; Brecht, M.; Ogata, H.; Higuchi, Y.; Lubitz, W. Single Crystal EPR Studies of the Reduced Active Site of [NiFe] Hydrogenase from Desulfovibrio Vulgaris Miyazaki F. *J. Am. Chem. Soc.* **2003**, *125* (1), 83–93.

(140) Sidabras, J. W.; Duan, J.; Winkler, M.; Happe, T.; Hussein, R.; Zouni, A.; Suter, D.; Schnegg, A.; Lubitz, W.; Reijerse, E. J. Extending Electron Paramagnetic Resonance to Nanoliter Volume Protein Single Crystals Using a Self-Resonant Microhelix. *Sci. Adv.* **2019**, *5* (10), eaay1394.

(141) Ash, P. A.; Carr, S. B.; Reeve, H. A.; Skorupskaite, A.; Rowbotham, J. S.; Shutt, R.; Frogley, M. D.; Evans, R. M.; Cinque, G.; Armstrong, F. A.; et al. Generating Single Metalloprotein Crystals in Well-Defined Redox States: Electrochemical Control Combined with Infrared Imaging of a NiFe Hydrogenase Crystal. *Chem. Commun.* **2017**, *53* (43), 5858–5861.

(142) Hinokuma, S.; Wiker, G.; Suganuma, T.; Bansode, A.; Stoian, D.; Huertas, S. C.; Molina, S.; Shafir, A.; Rønning, M.; van Beek, W.; et al. Versatile IR Spectroscopy Combined with Synchrotron XAS–XRD: Chemical, Electronic, and Structural Insights during Thermal Treatment of MOF Materials. *Eur. J. Inorg. Chem.* **2018**, *2018* (17), 1847–1853.

(143) Mulder, D. W.; Ratzloff, M. W.; Shepard, E. M.; Byer, A. S.; Noone, S. M.; Peters, J. W.; Broderick, J. B.; King, P. W. EPR and FTIR Analysis of the Mechanism of H2 Activation by [FeFe]-Hydrogenase HydA1 from Chlamydomonas Reinhardtii. *J. Am. Chem. Soc.* **2013**, *135* (18), 6921–6929.

(144) Zampella, G.; Fantucci, P.; De Gioia, L. Unveiling How Stereoelectronic Factors Affect Kinetics and Thermodynamics of Protonation Regiochemistry in [FeFe] Hydrogenase Synthetic Models: A DFT Investigation. *J. Am. Chem. Soc.* **2009**, *131* (31), 10909–10917.

(145) Haumann, M.; Stripp, S. T. The Molecular Proceedings of Biological Hydrogen Turnover. *Acc. Chem. Res.* **2018**, *51* (8), 1755–1763.

(146) Chapman, H. N.; Caleman, C.; Timneanu, N. Diffraction before Destruction. *Philos. Trans. R. Soc. B Biol. Sci.* **2014**, *369* (1647).

(147) Pandey, S.; Bean, R.; Sato, T.; Poudyal, I.; Bielecki, J.; Cruz Villarreal, J.; Yefanov, O.; Mariani, V.; White, T. A.; Kupitz, C.; et al. Time-Resolved Serial Femtosecond Crystallography at the European XFEL. *Nat. Methods* **2020**, *17* (1), 73–78.

(148) Fromme, P. XFELs Open a New Era in Structural Chemical Biology. *Nat. Chem. Biol.* **2015**, *11* (12), 895–899.

(149) Ash, P. A.; Reeve, H. A.; Quinson, J.; Hidalgo, R.; Zhu, T.; McPherson, I. J.; Chung, M. W.; Healy, A. J.; Nayak, S.; Lonsdale, T. H.; et al. Synchrotron-Based Infrared Microanalysis of Biological Redox Processes under Electrochemical Control. *Anal. Chem.* **2016**, *88* (13), 6666–6671.

(150) Armstrong, F. A.; Evans, R. M.; Hexter, S. V; Murphy, B. J.; Roessler, M. M.; Wul, P. Guiding Principles of Hydrogenase Catalysis Instigated and Clarified by Protein Film Electrochemistry. *Acc. Chem. Res.* **2016**, *49* (5), 884 – 892.

(151) Fourmond, V.; Wiedner, E. S.; Shaw, W. J.; Leger, C. On the Understanding and Design of Bidirectional and Reversible Catalysts of Multielectron, Multistep

Reactions. *J. Am. Chem. Soc.* **2019**, *141* (28), 11269–11285.

(152) Sensi, M.; Baffert, C.; Greco, C.; Caserta, G.; Gauquelin, C.; Saujet, L.; Fontecave, M.; Roy, S.; Artero, V.; Soucaille, P.; et al. Reactivity of the Excited States of the H-Cluster of FeFe Hydrogenases. *J. Am. Chem. Soc.* **2016**, *138* (41), 13612–13618.

(153) Garczarek, F.; Gerwert, K. Functional Waters in Intraprotein Proton Transfer Monitored by FTIR Difference Spectroscopy. *Nature* **2006**, *439*, 216–219.

(154) Debus, R. J. FTIR Studies of Metal Ligands, Networks of Hydrogen Bonds, and Water Molecules near the Active Site Mn4CaO5 Cluster in Photosystem II. *Biochim. Biophys. Acta - Bioenerg.* **2015**, *1847* (1), 19–34.

(155) Kottke, T.; Lórenz-Fonfría, V. A.; Heberle, J. The Grateful Infrared: Sequential Protein Structural Changes Resolved by Infrared Difference Spectroscopy. *J. Phys. Chem. B* **2017**, *121*, 335–350.

(156) Schultz, B.-J.; Mohrmann, H.; Lorenz-Fonfria, V. A.; Heberle, J. Protein Dynamics Observed by Tunable Mid-IR Quantum Cascade Lasers across the Time Range from 10 Ns to 1 S. *Spectrochim. Acta - Part A Mol. Biomol. Spectrosc.* **2017**, *188*, 666 – 674.

(157) Callender, R.; Dyer, R. B. Advances in Time-Resolved Approaches To Characterize the Dynamical Nature of Enzymatic Catalysis. *Chem. Rev.* **2006**, *106*, 3031–3042.

(158) Dyer, R. B.; Gai, F.; Woodruff, W. H.; Gilmanshin, R.; Callender, R. H. Infrared Studies of Fast Events in Protein Folding. *Acc. Chem. Res.* **1998**, *31* (11), 709–716.

(159) Lübben, M.; Gerwert, K. Redox FTIR Difference Spectroscopy Using Caged Electrons Reveals Contributions of Carboxyl Groups to the Catalytic Mechanism of Haem-Copper Oxidases. *FEBS Lett.* **1996**, *397* (2–3), 303–307.

(160) Gutman, M.; Nachliel, E. Time-Resolved Dynamics of Proton Transfer in Proteinous Systems. *Annu. Rev. Phys. Chem.* **1997**, *48* (1), 329–356.

(161) Greene, B. L.; Vansuch, G. E.; Chica, B. C.; Adams, M. W. W.; Dyer, R. B. Applications of Photogating and Time Resolved Spectroscopy to Mechanistic Studies of Hydrogenases. *Acc. Chem. Res.* **2017**, *50* (11), 2718–2726.

(162) Greene, B. L.; Wu, C. H.; McTernan, P. M.; Adams, M. W. W.; Dyer, R. B. Proton-Coupled Electron Transfer Dynamics in the Catalytic Mechanism of a [NiFe]-Hydrogenase. *J. Am. Chem. Soc.* **2015**, *137* (13), 4558–4566.

(163) Chica, B.; Wu, C. H.; Liu, Y.; Adams, M. W. W.; Lian, T.; Dyer, R. B. Balancing Electron Transfer Rate and Driving Force for Efficient Photocatalytic Hydrogen Production in CdSe/CdS Nanorod-[NiFe] Hydrogenase Assemblies. *Energy Environ. Sci.* **2017**, *10* (10), 2245–2255.

(164) Greene, B. L.; Wu, C.; Vansuch, G. E.; Adams, M. W. W.; Dyer, R. B. Proton Inventory and Dynamics in the Ni a -S to Ni a -C Transition of a [NiFe] Hydrogenase. *Biochemistry* **2016**, *55* (12), 1813–1825.

(165) Mirmohades, M.; Adamska-Venkatesh, A.; Sommer, C.; Reijerse, E.; Lomoth, R.; Lubitz, W.; Hammarström, L. Following [FeFe] Hydrogenase Active Site Intermediates by Time- Resolved Mid-IR Spectroscopy. *J. Phys. Chem. Lett.* **2016**, *7*, 3290–3293.

(166) Ratzloff, M. W.; Wilker, M. B.; Mulder, D. W.; Lubner, C. E.; Hamby, H.; Brown, K. A.; Dukovic, G.; King, P. W. Activation Thermodynamics and H/D Kinetic Isotope Effect of the Hox to H RedH+ Transition in [FeFe] Hydrogenase. *J. Am. Chem. Soc.* **2017**, *139*, 12879−12882.

(167) Greene, B. L.; Schut, G. J.; Adams, M. W. W.; Dyer, R. B. Pre-Steady-State Kinetics of Catalytic Intermediates of an [FeFe]-Hydrogenase. *ACS Catal.* **2017**, *7*, 2145–2150.

(168) Schut, G. J.; Adams, M. W. W. The Iron-Hydrogenase of Thermotoga Maritima Utilizes Ferredoxin and NADH Synergistically: A New Perspective on Anaerobic Hydrogen Production. *J. Bacteriol.* **2009**, *191* (13), 4451–4457.

(169) Sanchez, M. L. K.; Sommer, C.; Reijerse, E.; Birrell, J. A.; Lubitz, W.; Dyer, R. B. Investigating the Kinetic Competency of CrHydA1 [FeFe] Hydrogenase Intermediate States via Time-Resolved Infrared Spectroscopy. *J. Am. Chem. Soc.* **2019**, *141* (40), 16064–16070.

(170) Laun, K.; Baranova, I.; Duan, J.; Wittkamp, F.; Apfel, U.-P.; Happe, T.; Senger, M.; Stripp, S. T. Site-Selective Protonation of the Catalytic Cofactor in [FeFe]-Hydrogenase. *ChemRxiv* **2019**, under review.

(171) Reisner, E.; Powell, D. J.; Cavazza, C.; Fontecilla-Camps, J. C.; Armstrong, F. A. Visible Light-Driven H2 Production by Hydrogenases Attached to Dye-Sensitized TiO2 Nanoparticles. *J. Am. Chem. Soc.* **2009**, *131* (51), 18457–18466.

(172) Horch, M.; Lauterbach, L.; Saggu, M.; Hildebrandt, P.; Lendzian, F.; Bittl, R.; Lenz, O.; Zebger, I. Probing the Active Site of an O2-Tolerant NAD+-Reducing [NiFe]-Hydrogenase from Ralstonia Eutropha H16 by in Situ EPR and FTIR Spectroscopy. *Angew. Chemie Int. Ed.* **2010**, *49* (43), 8026–8029.

(173) Mészáros, L. S.; Németh, B.; Esmieu, C.; Ceccaldi, P.; Berggren, G. In Vivo EPR Characterization of Semi-Synthetic [FeFe] Hydrogenases. *Angew. Chemie - Int. Ed.* **2018**, *57* (10), 2596–2599.

(174) Kamp, C.; Silakov, A.; Winkler, M.; Reijerse, E. J.; Lubitz, W.; Happe, T. Isolation and First EPR Characterization of the [FeFe]-Hydrogenases from Green Algae. *Biochim. Biophys. Acta* **2008**, *1777* (5), 410–416.

(175) Barstow, B.; Agapakis, C. M.; Boyle, P. M.; Grandl, G.; Silver, P. A.; Wintermute, E. H. A Synthetic System Links FeFe-Hydrogenases to Essential E. Coli Sulfur Metabolism. *J. Biol. Eng.* **2011**, *5*, 1–15.

(176) Wegelius, A.; Khanna, N.; Esmieu, C.; Barone, G. D.; Pinto, F.; Tamagnini, P.; Berggren, G.; Lindblad, P. Generation of a Functional, Semisynthetic [FeFe]-Hydrogenase in a Photosynthetic Microorganism. *Energy Environ. Sci.* **2018**, *11* (11), 3163–3167.

(177) Poudel, S.; Tokmina-Lukaszewska, M.; Colman, D. R.; Refai, M.; Schut, G. J.; King, P. W.; Maness, P. C.; Adams, M. W. W.; Peters, J. W.; Bothner, B.; et al. Unification of [FeFe]-Hydrogenases into Three Structural and Functional Groups. *Biochim. Biophys. Acta - Gen. Subj.* **2016**, *1860* (9), 1910–1921.

(178) Appel, J.; Hueren, V.; Boehm, M.; Gutekunst, K. Cyanobacterial in Vivo Solar Hydrogen Production Using a Photosystem I – Hydrogenase. *Nat. Energy* **2020**, in press.

(179) Lichtman, J. W.; Conchello, J. A. Fluorescence Microscopy. *Nat. Methods* **2005**, *2* (12), 910–919.

(180) Wencel, D.; Abel, T.; McDonagh, C. Optical Chemical PH Sensors. *Anal. Chem.* **2014**, *86* (1), 15–29.

(181) Kos, P.; Plenio, H. A Fluorescent Molecular Probe for the Detection of Hydrogen Based on Oxidative Addition Reactions with Crabtree-Type Hydrogenation Catalysts. *Angew. Chemie - Int. Ed.* **2015**, *54* (45), 13293–13296.

(182) Amrania, H.; Drummond, L.; Coombes, R. C.; Shousha, S.; Woodley-Barker, L.; Weir, K.; Hart, W.; Carter, I.; Phillips, C. C. New IR Imaging Modalities for Cancer Detection and for Intra-Cell Chemical Mapping with a Sub-Diffraction Mid-IR s-SNOM. *Faraday Discuss.* **2016**, *187*, 539–553.

(183) Jin, M.; Lu, F.; Belkin, M. A. High-Sensitivity Infrared Vibrational Nanospectroscopy in Water. *Light Sci. Appl.* **2017**, *6* (7), e17096.

(184) Amenabar, I.; Poly, S.; Goikoetxea, M.; Nuansing, W.; Lasch, P.; Hillenbrand, R. Hyperspectral Infrared Nanoimaging of Organic Samples Based on Fourier Transform Infrared Nanospectroscopy. *Nat. Commun.* **2017**, *8*, e14402.

(185) Kochan, K.; Perez-Guaita, D.; Pissang, J.; Jiang, J. H.; Peleg, A. Y.; McNaughton, D.; Heraud, P.; Wood, B. R. In Vivo Atomic Force Microscopy-Infrared Spectroscopy of Bacteria. *J. R. Soc. Interface* **2018**, *15*, e0115.

(186) del Barrio, M.; Sensi, M.; Orain, C.; Baffert, C.; Dementin, S.; Fourmond, V.; Léger, C. Electrochemical Investigations of Hydrogenases and Other Enzymes That Produce and Use Solar Fuels. *Acc. Chem. Res.* **2018**, *51* (3), 769–777.

(187) Horch, M.; Schoknecht, J.; Wrathall, S. L. D.; Greetham, G. M.; Lenz, O.; Hunt, N. T. Understanding the Structure and Dynamics of Hydrogenases by Ultrafast and Two-Dimensional Infrared Spectroscopy. *Chem. Sci.* **2019**, *10* (39), 8981–8989.

(188) Adamson, H.; Robinson, M.; Bond, P. S.; Soboh, B.; Gillow, K.; Simonov, A. N.; Elton, D. M.; Bond, A. M.; Sawers, R. G.; Gavaghan, D. J.; et al. Analysis of HypD Disulfide Redox Chemistry via Optimization of Fourier Transformed Ac Voltammetric Data. *Anal. Chem.* **2017**, *89* (3), 1565–1573.